



**STUDY OF MORPHOLOGY AND BONDING
BEHAVIOUR OF TORREFIED BIOCHAR FROM
OIL PALM EMPTY FRUIT BUNCH**

by

NOR AIN FATIHAH MOHD AZIZI

A report submitted in fulfillment of the requirements for the degree of
Bachelor of Applied Science (Sustainable Science) with Honours

**FACULTY OF EARTH SCIENCE
UNIVERSITI MALAYSIA KELANTAN**

2019

DECLARATION

I declare that this thesis entitled “A Study of Morphology and Bonding Analysis of Torrefied Biochar from Oil Palm Empty Fruit Bunch (OPEFB)” is the result of my own research except as cited in the references. The thesis has not been accepted for my degree and is not concurrently submitted in candidature of any other degree.

Signature: _____

Name : NOR AIN FATIHAH MOHD AZIZI

Date : 10/12/2018

UNIVERSITI
MALAYSIA
KELANTAN

ACKNOWLEDGEMENT

Alhamdulillah. Thanks to Allah SWT, whom with His willing giving me the opportunity to complete this Final Year Project. Firstly, I would like to express my deepest thanks to Dr Mohamad Faiz bin Mohd Amin who assigned as my supervisor, Mohd Sukhairi Mat Rasat as my research team leader, who had guided me a lot of task during two semesters session 2018/2019.

I also want to thanks the lecturers and staffs of Faculty of Earth Science for their cooperation during I complete the final year project that had given valuable information, suggestions and guidance in the compilation and preparation this final year project report.

Deepest thanks and appreciation to my parents, family, special mate of mine, and others for their cooperation, encouragement, constructive suggestion and full of support for the report completion, from the beginning till the end. Also thanks to all of my friends and everyone, that have been contributed by supporting my work and help myself during the final year project progress till it is fully completed.

A Study of Morphology and Bonding Analysis of Torrefied Biochar from Oil Palm Empty Fruit Bunch (OPEFB)

ABSTRACT

Considering the global energy crisis that affect the worldwide consumers on the insufficiency of fossil fuel and specific interest to invent alternative renewable energy sources. This study was conducted to identify the potential of torrefied OPEFB biochar as a renewable energy sources by underwent torrefaction process based on particle size, holding temperature and residence time. The process have been carried out within holding temperature varied from 200 to 300°C in the absence of oxygen under low heating rate by using furnace in 30 to 90 minutes of their residence time, respectively. In brief, this study focused on the optimization by using the response surface method (RSM), Box-Benhken Model and the analysis of morphology as well as the bonding behavior of the torrefied OPEFB biochar due to its properties and functional groups in order to enhance the potential of the OPEFB as renewable energy sources by the aids of Scanning Electron Microscope (SEM) and Fourier Transformation Infrared Spectroscopy (FTIR). SEM images showed the surface morphology of OPEFB after undergo torrefaction by which it was completely decomposed by initiating pores while the structure become flattened with almost left sharp edge compared to the raw EFB. The changes of presence functional groups before and after the torrefaction process were observed under certain wavelength which were C=O (1750-1680 cm^{-1}), N-H (3500-3100 cm^{-1}) and C-N (1350-1000 cm^{-1}). These functional groups determined the changes of functional groups as well as the wavelength whereby the degradation of hemicellulose, cellulose and lignin take place.

UNIVERSITI
MALAYSIA
KELANTAN

Kajian Morfologi dan Analisis Ikatan Keatas *Torrefied Biochar* daripada Tandan Buah Kosong Kelapa Sawit (OPEFB)

ABSTRAK

Memandangkan krisis tenaga global yang memberi kesan kepada pengguna di seluruh dunia pada kekurangan bahan api fosil dan kepentingan tertentu untuk mencipta alternatif baru sumber tenaga boleh diperbaharui. Kajian ini telah dijalankan untuk mengenal pasti potensi *biochar* daripada tandan buah kosong kelapa sawit (OPEFB) sebagai sumber tenaga boleh diperbaharui oleh proses torrefaction berdasarkan saiz, suhu dan masa. Proses ini telah dilaksanakan dalam tempoh suhu dari 200 hingga 300°C dalam ketiadaan oksigen di bawah kadar suhu pemanasan yang rendah dengan menggunakan relau dalam 30 hingga 90 minit. Secara ringkasnya, kajian ini memberi tumpuan kepada pengoptimuman dengan menggunakan kaedah gerak balas permukaan (RSM), Box-Benhken Model dan analisis morfologi serta ciri ikatan *torrefied OPEFB biochar* keatas ciri-ciri dan kumpulan berfungsi bagi meningkatkan potensi OPEFB sebagai sumber tenaga boleh diperbaharui oleh bantuan daripada Mikroskop Imbasan Elektron (SEM) dan Transformasi Fourier Inframerah Spektroskopi (FTIR). Imej SEM menunjukkan morfologi permukaan OPEFB selepas menjalani torrefaction yang mana ia mengalami pereputan keseluruhan dalaman melalui penghasilan liang roma seterusnya menjadikan struktur leper dengan tepi yang tajam berbanding OPEFB mentah. Perubahan kehadiran kumpulan berfungsi sebelum dan selepas proses torrefaction yang diperhatikan di bawah panjang gelombang tertentu yang menjadi C=O (1750-1680 cm^{-1}), N-H (3500-3100 cm^{-1}) dan C-N (1350-1000 cm^{-1}). Kumpulan-kumpulan ini berfungsi menentukan di mana degradasi hemiselulosa, selulosa dan lignin berlaku.

UNIVERSITI
MALAYSIA
KELANTAN

TABLE OF CONTENTS

	PAGE
DECLARATION	ii
ACKNOWLEDGEMENT	iii
ABSTRACT	iv
ABSTRAK	v
TABLE OF CONTENT	vi
CHAPTER 1 INTRODUCTION	1
1.1 Background of Study	1
1.2 Problem Statement	3
1.3 Objectives	4
1.4 Scope of Study	4
CHAPTER 2 LITERATURE REVIEW	5
2.1 Overview of Energy	5
2.1.1 Energy Crisis	6
2.1.2 Energy Policies/ Status in Malaysia	7
2.1.3 Energy Consumption	10
2.2 Renewable Energy	14
2.2.1 Biomass Energy	15
2.3 Biomass Sources from Oil Palm Plantation	16
2.3.1 Oil Palm in Malaysia	18
2.4 Thermochemical Energy Conversion	19
2.5 Torrefaction Process	20
2.6 Response Surface Methodology	21
2.7 Optimization and Properties of Torrefied OPEFB Biochar	22
2.8 Morphological Characterization	24
2.9 Bonding Behaviour Characterization	25
2.9.1 Characteristic IR Absorption Frequencies of Organic Functional Groups	27
CHAPTER 3 MATERIALS AND METHOD	29
3.1 Materials	29
3.1.1 Sample Preparation	29
3.2 Methods	32
3.2.1 Torrefaction Process	32
3.2.2 Optimization	32
3.2.3 Characterization Analysis	36

3.3	Data Analysis	37
	CHAPTER 4 RESULTS AND DISCUSSION	38
4.1	Physical Appearance of Raw and Torrefied OPEFB Biochar	38
4.2	Mass Yield of Torrefied OPEFB Biochar	39
4.3	Proximate Properties for Raw and Torrefied OPEFB Biochar	41
4.3.1	Moisture Content	41
4.3.2	Volatile Matter	42
4.3.3	Ash Content	43
4.3.4	Fixed Carbon	44
4.4	Energy Content	45
4.5	Optimization of Raw and Torrefied OPEFB Biochar	46
4.6	Morphology Properties of Raw and Torrefied OPEFB Biochar	50
4.7	Bonding Properties of Raw and Torrefied OPEFB Biochar	54
	CHAPTER 5 CONCLUSION AND RECOMMENDATIONS	61
5.1	Conclusion	61
5.2	Recommendations	61
	REFERENCES	63
	APPENDIX-A	69
	APPENDIX-B	Error! Bookmark not defined.

LIST OF TABLES

NO.		PAGE
2.1	Statistic of installed electric capacity in Malaysia in 2016	27
2.2	Distribution of oil palm planted area by category in Malaysia 2017	32
2.3	Properties of raw OPEFB	35
2.4	Proximate analysis results of OPEFB biochar	36
2.5	Chemical composition of oil palm	39
2.6	IR Absorption Frequencies of Organic Functional Groups	40
4.1	ANOVA for calorific value	46
4.2	Optimum condition suggested by RSM	49

LIST OF FIGURES

NO.		PAGE
2.1	Chronology of energy policies in Malaysia	23
2.2	The World GDP, electricity generation and electricity consumption for 1980-2014 period	24
2.3	World gross electricity production by source in 2016	24
2.4	Energy consumption of electricity by region 2017	25
2.5	The GDP, electricity generation and electricity consumption trends in Malaysia for 1980-2014	26
2.6	Total installed electric capacity in Malaysia	27
2.7	Fresh fruit bunches monthly yield in 2016-2017	30
2.8	SEM images (a, b, c, d and e) of OPEFB biochar with magnification of x2500	37
3.1	(a) Raw OPEFB and (b) OPEFB fibre used for torrefaction	42
3.2	The overall process of torrefied OPEFB biochar	44
4.1	Samples of Raw and Torrefied OPEFB Biochar	52
4.2	Effect of holding temperature and residence time on the mass yield	53
4.3	Effect of holding temperature and residence time on moisture content	54
4.4	Effect of holding temperature and residence time on volatile content	55
4.5	Effect of holding temperature and residence time on ash content	56
4.6	Effect of holding temperature and residence time on fixed carbon	57
4.7	Effect of holding temperature and residence time on calorific value	58
4.8	Correlation between the actual and predicted values for of the torrefied OPEFB biochar optimization on calorific value	60
4.9	Response surface 3D curve of the torrefied OPEFB biochar optimization on its calorific value	61
4.10	SEM images of raw OPEFB surface structure sieved 500 μ m (a) magnification x250, (b) magnification x1500, (c) magnification	62

	x5000	
4.11	SEM images of torrefied OPEFB biochar surface structure on 30 minutes of torrefaction at respective holding temperatures with magnifications of x250 (a, d and g), x1500 (b, e and h) and x5000 (c, f and i)	63
4.12	SEM images of torrefied OPEFB biochar surface structure on 60 minutes of torrefaction at respective holding temperatures with magnifications of x250 (a, d and g), x1500 (b, e and h) and x5000 (c, f and i)	64
4.13	SEM images of torrefied OPEFB biochar surface structure on 90 minutes of torrefaction at respective holding temperature temperatures with magnifications of x250 (a, d and g), x1500 (b, e and h) and x5000 (c, f and i)	65
4.14	Functional groups presence during 30 minutes of torrefaction	67
4.15	Functional groups presence during 60 minutes of torrefaction	69
4.16	Figure 4.16: Functional groups presence during 90 minutes of torrefaction	71

LIST OF ABBREVIATIONS

EFB	Empty Fruit Bunch
CPO	Crude Palm Oil
OPEFB	Oil Palm Empty Fruit Bunch
MPOB	Malaysian Palm Oil Board
BP	British Petrol
H/C	Hydrogen-to-Carbon
O/C	Oxygen-to-Carbon
PSC	Production Sharing Contracts
FTIR	Fourier Transformation Infrared
SEM	Scanning Electron Microscope
BSE	Backscattered Electron
SE	Secondary Electron
IR	Infrared
CO ₂	Carbon dioxide
GHGs	Greenhouse gases
OPT	Oil palm trunk
OPF	oil palm fronds
EFB	empty fruit bunch
PKS	palm kernel shell
MF	mesocarp fibre
POME	palm oil mill effluent
RSM	Response surface method
EPU	Economic Planning Unit
EIA	Energy Information Administration
NEB	National Electricity Board
SREP	Small Renewable Energy Program
OECD	Organisation of Economic Co-operation and Development
EWS	Efficient World Scenario
M _Y	Mass yield
MC	Moisture content

VM	Volatile matter
AC	Ash content
FC	Fixed Carbon
LSSPV	large-scale solar photovoltaic
GNI	Gross National Income



LIST OF SYMBOLS

%	Percentage
°C	Degree Celcius
Mtoe	Million Tonnes of Oil Equivalent
MW	Megawatt
bb/d	Barrels per Day
kg	Kilogram
MJ/kg	Megajoules per Kilogram
cm	Centimeter
mL min ⁻¹	Millilitre per Minute
cm ⁻¹	Wavenumber

UNIVERSITI
MALAYSIA
KELANTAN

CHAPTER 1

INTRODUCTION

1.1 Background of Study

Considering the non-renewable nature of fossil fuel, insufficiency of fossil fuel and the unstable in fossil fuel price, especially for oil, specific interest to invent alternative renewable fuel remains relevant. Also, the over dependence of the chemical industries on petrochemicals raw materials especially organic chemicals produced from petroleum feedstock had placed much demand on fossil fuel (MPOB, 2018a) . The dismissive impact of fossil fuel to the environment is enormous, particularly as it leads in rising of greenhouse gases (GHGs) level in the atmosphere, and its associated global warming effect. Fossil fuel combustion accounts for about 90% of carbon dioxide (CO₂) which is the major contributor to GHGs (Rahman et al., 2014). The expected environmental destruction due to emissions from combustion of fossil fuel has become a critical issue. Therefore, it necessitated a shift from the use of non-renewable fossil fuel as source of energy to utilizing renewable energy sources such as biomass with less environmental detrimental effects and continually generated.

Biomass can either be from wood and agricultural residues, yard and municipal wastes, landfill gas or alcohol fuels. In most cases, biomass is left to decompose in the fields such as food wastes, animal waste, corn stover, rice husk and oil palm waste. But in this case, the biomass referred was the agricultural by-products generated from the oil palm industries during replanting, pruning and milling activities. About 90% is

predominantly considered as biomass, palm oil only accounts for 10% of the tree (Kurnia et al., 2016). Oil palm biomass generated at the plantation includes oil palm trunk (OPT) and oil palm fronds (OPF), meanwhile biomass from empty fruit bunch (EFB), palm kernel shell (PKS), mesocarp fibre (MF) and palm oil mill effluent (POME) is generated at the oil palm processing mills (Samiran et al., 2015).

There were numerous benefits embedded in biomass, but before these benefits can be exploited fully, the biomass must be subjected to certain pretreatments (Mulakhudair et al., 2017). Hence, the need to convert biomass into useful materials with minimal environmental challenges became imminent. There were wide range of technologies available for converting biomass to value added products such as biofuels, biochemical, syngas and biochar include chemical, physical, thermochemical and biochemical conversions respectively. Biomass that converted to energy via thermochemical routes involved three main process combustion, gasification and pyrolysis. While pyrolysis can either be conducted very slowly or rapidly, which defined the type of pyrolysis such as torrefaction (mild-pyrolysis).

In the light of this, the pretreatment techniques mentioned such as torrefaction, enhanced the utilization and conversion efficiency of biomass resources. Torrefaction process in which biomass was treated in the temperature range from 200 to 300°C in a non-oxidising environment (Bevan et al., 2018). The drying and partial devolatilization of biomass during torrefaction reduced the mass of biomass without affecting the energy content and the torrefaction improved the solid fuel properties of biomass by depolymerising long chain polysaccharide and removing CO₂ and water (H₂O). Hence, by reducing the oxygen-to-carbon (O/C) ratio, the energy density and hygroscopic nature of biomass is significantly enhanced (Basu, 2013).

1.2 Problem Statement

Analogy to global energy situation, Malaysia has faced to the problem of energy crisis, where Malaysia mainly depends on non-renewable energy sources such as fossil fuel for electricity generation. Due to the depletion and environmental concerns, governments are forced to consider appropriate alternative electricity resources for sustainable energy.

Since Malaysia is the agricultural base country, there were a lot of agricultural crops such as oil palm. During the harvesting and processing of these agricultural crops, some residues are left over, for example oil palm empty fruit bunch (OPEFB). These residues can further be used as the substitute to fossil fuel for energy production and consequently, can solve the problem of energy crisis as well as global warming by undergo torrefaction process.

Therefore, this study seeks to examine the effect of torrefaction on the morphology and bonding analysis of torrefied biochar from OPEFB from mild to severe holding temperature conditions ranging from 200 to 300°C with 30, 60 and 90 minutes of residence time. It have been examined the morphology reaction conditions, bonding properties and potential product yield from the torrefied OPEFB biochar through scanning electron microscope (SEM) and fourier transformation infrared spectroscopy (FTIR). The technique was a simple, timely and reliable approach widely applied to simulate and examine the thermochemical biomass conversion processes such as torrefaction in the literature (Chew et al., 2016).

1.3 Objectives

- i. To identify the optimization of the torrefied OPEFB biochar energy content by using response surface method (RSM), Box-Benhken model according to OPEFB particle size, holding temperature and residence time of the torrefaction process.
- ii. To analyse the morphology and bonding behaviour of the torrefied OPEFB biochar by using SEM and FTIR.

1.4 Scope of Study

This study was conduct to identify the potential of OPEFB as a renewable energy sources by undergo torrefaction process based on three independent variable which is particle size, holding temperature and residence time. During the torrefaction process, there were three different particle sizes (250, 500 and 750 μ m) of OPEFB were heated to about 200 to 300 $^{\circ}$ C for 30, 60 and 60 minutes of their residence time. In brief, this study focused on the optimization and the morphology also bonding behaviour of the torrefied OPEFB biochar due to its properties and functional groups also in order to enhance the potential of the product. Meanwhile, the limitation of the study was the main product from this process was the biochar instead of the biofuel or biosyngas. It is because the yields of these three fractions varied significantly depended upon the process condition (Cheng, 2014).

CHAPTER 2

LITERATURE REVIEW

2.1 Overview of Energy

In Asian country, electricity generation and consumption are one of the most vital issues. Currently, 97.6% of Malaysian have access to electricity in several sectors like manufacturing, construction, transportation and housing (EPU, 2016). Realizing the rise in electricity consumption, the government incessantly reviews its energy policy to make sure long-term reliability and security of energy resources and to satisfy the electricity demand, all countries have resorted to the utilization of energy resources for generating electricity to extend their installed capability (Hussain, 2016).

At present, most countries around the world rely on non-renewable energy for electricity generation. In Malaysia, the power system relies primarily on non-renewable energy to meet its electricity consumption needs. Malaysia therefore, considered the use of non-renewable energy products and subsequently increased energy dependency. With the rise in non-renewable energy prices and the global concern to reduce GHGs, the demand for the shift from CO₂ producing non-renewable energy to renewable electricity sources is growing.

This case proves that non-renewable energy sources cannot meet the growing demand for energy and the solution to the crisis lies in the use and sustainability of renewable energy sources for power generation. Ultimately, oriented efforts are being made to ensure the sustainability of energy sources.

2.1.1 Energy Crisis

Presently, the energy crisis poses the real threat to sustainability for developing countries, just as their energy consumption grows faster than developed countries. Fossil fuels, on the other hand, can no longer be sustained in the near future due to environmental impacts and the depletion of reserves. As a result, it became one of the most urgent actions the whole world had to encounter.

The energy crisis is a consequence of many different pressures on our natural resources, not only one. Due to over consumption, there is a strain on fossil fuels which can then affect our water and oxygen resources by causing pollution. The steady growth of the world's population and its demands for fuel and products was another cause of the crisis. No matter what type of food or products chosen to use in a sweatshop from fair trade and organic products, not one of them is produced or transported without a significant drain on the energy resource. Renewable energy is still unused for the most part.

The majority of the energy originates from non-renewable sources such as coal. It is still the top choice to generate energy. Renewable sources of energy can reduce our dependence on fossil fuels and also reduce emissions of greenhouse gases. Thus, in recent decades the energy crisis has become a serious threat to sustainability, especially in developing countries and communities.

Since natural gas has been used to meet the prolonged demand for electricity, Malaysia has become a traditional exporter of liquid natural gas (LNG) because it is a significant producer of natural gas and has a strategic location for the seaborne energy trade. Malaysia became the second biggest exporter of LNG in the world after Qatar in 2012 (EIA, 2013). However, Malaysia currently threatened a scarcity of renewable sources due to its demand and rapid economic growth.

2.1.2 Energy Policies/ Status in Malaysia

Over the years, the Malaysian government has developed numerous energy-related policies to ensure the long-term security and reliability of the energy supply for the country's sustainable social and economic development. Energy policies and strategies to protect the use of non-renewable energy have also been highlighted, with a focus on the various energy sources available for high and sustained growth. The focus was also on the role of renewable energy as an alternative source for increasing the security of electricity supply (Hamdi et al., 2014). For the past 60 years, Malaysia's government has developed a number of energy related policies to ensure sustainability and security of energy supply. The first policy dates back to 1949, when the Central Electricity Board (CED) was first formed before it was converted into the National Electricity Board (NEB) in 1965 (Tick et al., 2010).

The first policy that really impacted the industry was the Petroleum Development Act 1974, vested on PETRONAS, the state-owned oil and gas company, the exclusive rights to explore, develop and produce petroleum resources in Malaysia, followed by the National Petroleum policy 1975 to regulate downstream oil and gas industry via the Petroleum Regulations 1974. The more significant policy, the National Energy Policy was actually introduced in 1979 with three primary objectives which are supply, utilization and environmental. The first objective is to ensure the provision of adequate, secure, and cost-effective energy supplies through developing indigenous energy resources both non-renewable and renewable energy resources using the least cost options and diversification of supply sources both from within and outside the country. The second objective is to promote the efficient utilization of energy and to discourage wasteful and non-productive patterns of energy consumption, and the last

objective is aimed to minimize the negative impacts of energy through efficient energy utilization.

After that, the National Depletion Policy 1980 and a year later, the Four-Fuel Diversification Strategy 1981 were implemented, with the former to prolong lifespan of the country's oil reserves for future security and stability of oil supply and the latter to pursue balanced utilization of natural gas, oil, hydro and coal. The fuel diversification policy in Malaysia is reviewed from time to time to ensure that the country is not over-dependent on one main energy source, especially after the two occurrences of international oil crisis in 1973 and 1979.

The policy was further revised in 1999 with the announcement of the Five-Fuel Diversification Strategy. Renewable energy (RE) was made the fifth fuel in the energy supply mix with the target to contribute 5% of the country's electricity demand by year 2005. In order to meet this goal, the Small Renewable Energy Program (SREP) was launched in May 2001 under the initiative of the Special Committee on Renewable Energy (SCORE) aimed to support the government's strategy in intensifying the development and utilization of RE as the fifth fuel resource in power generation, which is also stipulated in the objectives of the Third Outline Perspective Plan (OPP) for 2001–2010 and the 8th Malaysia Plan (2001–2005).

The primary focus of SREP is to facilitate the expeditious implementation of grid connected RE resource-based small power plants. In the 9th Malaysian Plan (2006–2010), the emphasis on energy efficiency is intensified to address the nation's energy challenge in line with the sustainable development agenda. Before the Five-Fuel Diversification Strategy in 1999, oil made up a large portion of the country's energy mix for the past few decades. After faced with the possibility of

prolonged energy crisis back in the 1970s, other options of energy resources such as natural gas, coal and hydro became viable, as natural gas and hydro were largely untapped then, and coal was considered a plentiful and reliable worldwide resource with low and stable price (KeTTHA, 2017) . The policy drivers and legislative framework in Malaysia has been continued to evolve to better address the country's energy needs and development. Policies that were introduced since then have been covered quite extensively and summarized in Figure 2.1.

<p>Petroleum Development Act 1974</p>	<ul style="list-style-type: none"> • Vested on PETRONAS the exclusive rights to explore, develop and produce petroleum resources of Malaysia
<p>National Petroleum Policy 1975</p>	<ul style="list-style-type: none"> • Efficient utilization of petroleum resources • Ensuring the nation exercises majority control in the management and operation of the industry
<p>National Energy Policy 1979</p>	<ul style="list-style-type: none"> • Ensure adequate, secure and cost-effective supply • Promote efficient utilization of energy and eliminate wasteful and non-productive usage
<p>National Depletion Policy 1980</p>	<ul style="list-style-type: none"> • To prolong the life span of the nation's oil and gas reserves
<p>Four-fuel Diversification Strategy 1981</p>	<ul style="list-style-type: none"> • Aimed at ensuring reliability and security of supply through deversification of fuel (oil, natural gas, hydro and coal)
<p>Five-fuel Diversification Strategy 1999</p>	<ul style="list-style-type: none"> • Renewable energy included as the "fifth fuel" in energy supply mix
<p>Small Renewable Energy Power (SREP) Programme 2001</p>	<ul style="list-style-type: none"> • Encourage small private power generation projects using renewables

KELANTAN

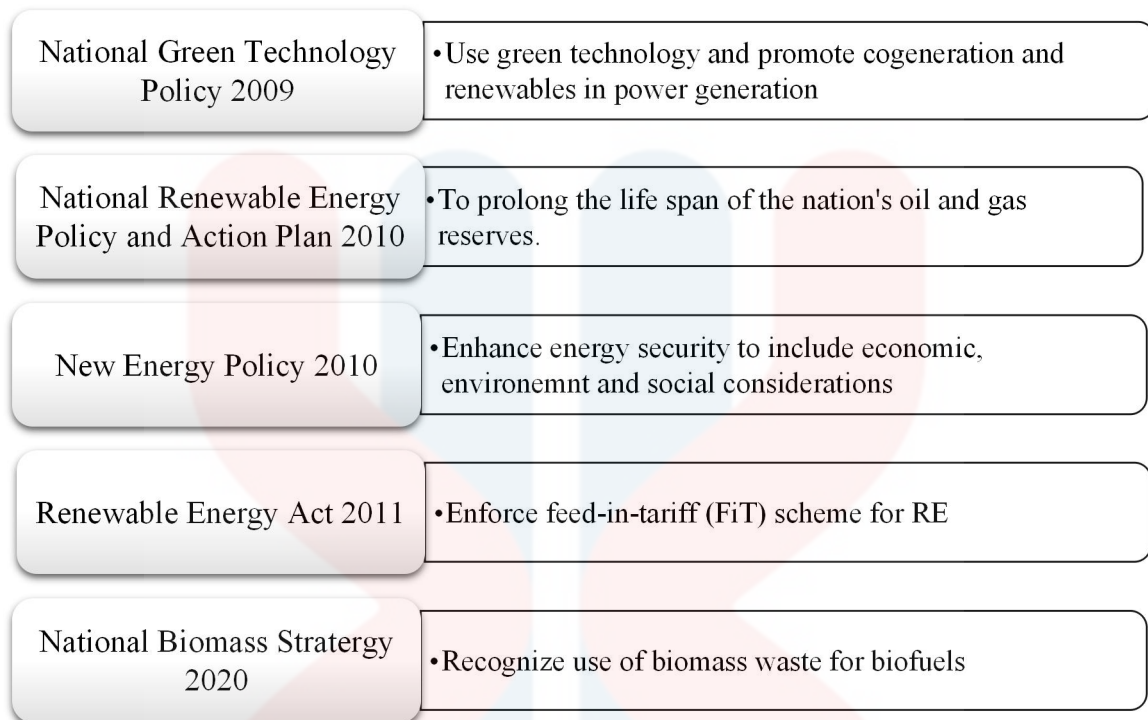


Figure 2.1: Chronology of energy policies in Malaysia
(Sources: KeTTHA, 2017)

It is now clear that in order to achieve sustainable development through renewable energy, energy policies and strategies, government, industries and individual or community participation must be well specifically designed and supported. The expectation was to have a detrimental effect on sustainable development through renewable sources for present and future generations (Hussain & Hamisham, 2016).

2.1.3 Energy Consumption

The world's gross electricity output was 2.9% higher in 2016 than in 2015. Since 1974, global electricity production has grown steadily over the years, except between 2008 and 2009, when the economic crisis in the Organisation of Economic Co-operation and Development (OECD) countries has led to a visible drop in global

production. In 2014, the total gross domestic product (GDP) was more than RM 50 billion as stated in Figure 2.2 while in 2016, generation from combustible fuels also accounted for 67.3% of total world gross energy consumption (IEA, 2018).

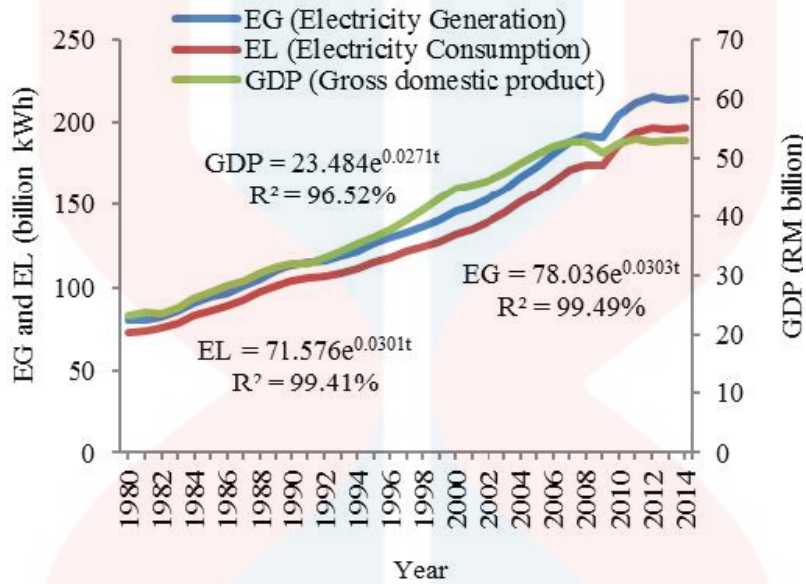


Figure 2.2: The World GDP, electricity generation and electricity consumption for 1980-2014 period (Source: EIA, 2015)

Combustible fuels include coal and coal products, oil and oil products, natural gas, biofuels including solid biomass and animal products, gas/liquids from biomass, industrial waste and municipal waste. The world gross electricity production by energy source in 2016 also portrayed coal was the highest usage as shown in Figure 2.3.

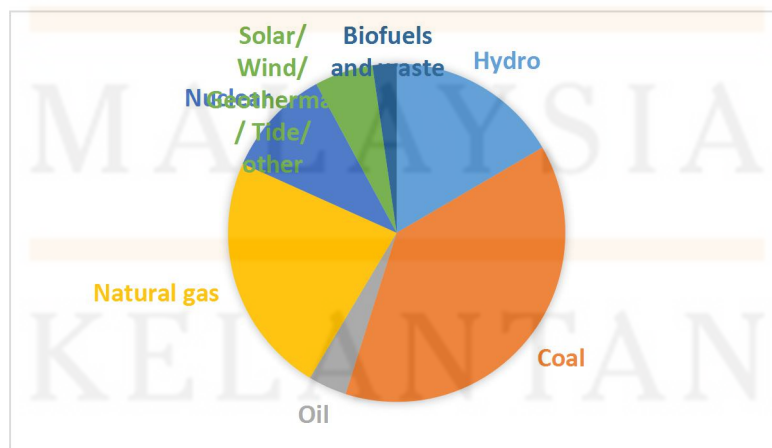


Figure 2.3: World gross electricity production by energy source in 2016 (Source: ST, 2016)

The Efficient World Scenario (EWS) identifies the industry's potential to generate almost twice as much value per unit of energy consumption in 2040 as it does today. The overall manufacturing energy intensity could improve by 44% in less energy intensive manufacturing sectors by 2040 with 70% of the energy saving potential (IEA), 2018).

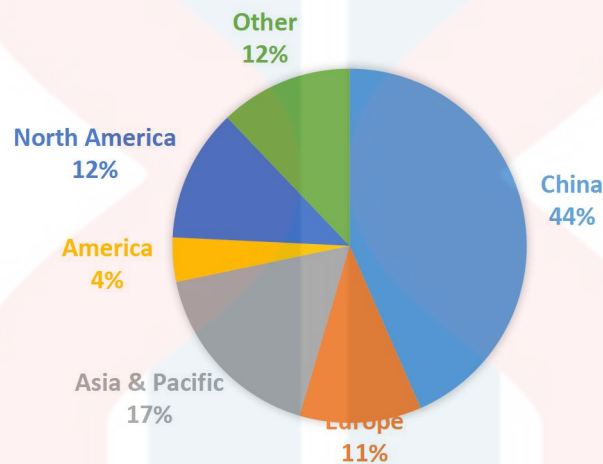


Figure 2.4: Energy consumption of electricity by region 2017 (Source: IEA, 2018)

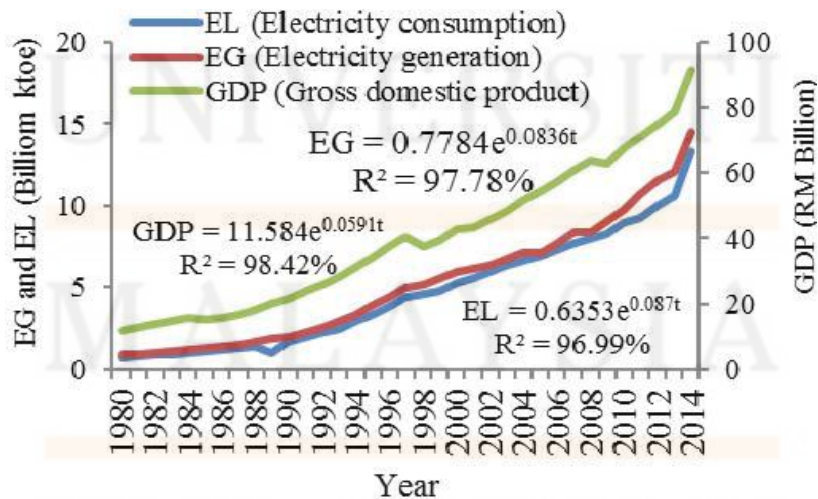


Figure 2.5: The GDP, electricity generation and electricity consumption trends in Malaysia for 1980-2014 (Source: ST, 2015).

In Malaysia, electricity demand which is mainly fulfilled by natural gas and coal has continued to expand rapidly over the years. According to Figure 2.6, the total installed capacity at present stands at around 29,253 gigawatt (GW), with most of the power stations located in the more densely populated and industrialized Peninsular Malaysia. The states of Sabah and Sarawak which are located in the Borneo are mostly powered up by hydropower due to their favourable geographical terrains. Some of these gas-fired plants are capable to run on two fuels and this has allowed greater flexibility in fuel selection and usage. Total installed capacity in Malaysia in 2016 was recorded in Table 2.1.

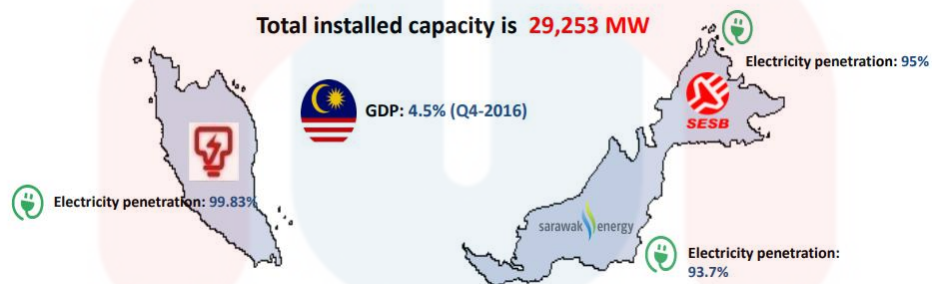


Figure 2.6: Total installed electric capacity in Malaysia
(Source from :KeTTHA, 2017)

Table 2.1: Statistic of installed electric capacity in Malaysia in 2016
(Source from :KeTTHA, 2017)

As of 2016	Installed	Peak Demand	Reserve Margin
	Capacity (MW)	(MW)	(%)
Pen. Malaysia	23,249	17,788	28.7
Sabah	1567	944.9	37.9
Sarawak	4437	3,315	34

2.2 Renewable Energy

Malaysia relies primarily on non-renewable energy sources such mostly coming from fossil fuel to generate electricity. Electricity plays a major role in society's well-being and social prosperity in countries. The electricity demand is growing and the trend is likely to continue globally in the future (Hussain & Hamisham, 2016). Due to environmental concerns, multiple approaches for generating electricity for sustainable energy have been generally considered. In Malaysia, therefore renewable sources such as hydro, solar, biogas and biomass were made up of the electricity industry.

Malaysia has also devoted itself to taking into account renewable sources of energy in the electricity generation mix. The 2020 climate energy package seeks to make Malaysia energy efficient by reducing CO₂ emissions by 40% (EPU, 2016).

The government has targeted a 5% of RE in the energy mix by 2010 when the Five-Fuel Diversification Policy was announced during the 8th Malaysian Plan (8MP) from 2001 to 2005, but only 1.8% was achieved. At present, the contribution from RE in the mix is estimated at roughly 1%. Since the FiT scheme introduced in 2011, 5,777 RE projects have been commissioned with an installed capacity of about 326.05 MW from a total licensed capacity of 358.23 MW that mostly went to solar (187.17 MW) and followed by biomass (114.93 MW), mini hydro (29.88 MW) and lastly biogas (26.25 MW). An average hike of 14.89% of the electricity tariff in January 2014 had ignited the awareness of consumers towards electricity usage and the importance of energy savings and efficiency (TNB, 2016).

Implementation of RE projects have intensified since, with the government awarding several large-scale solar photovoltaic (LSSPV) contracts by the end of 2016 which shall contribute significantly to the overall generation mix once these solar

fields are up and running. In terms of installed capacity, the cumulative annual growth rate of RE capacity towards 2020 as envisioned by the government as part of the 11MP, is expected to exceed 11% to achieve at least 2080 MW, coming from mini hydro, biomass biogas and solar. RE share in overall fuel mix is projected to gradually increase to 3% of total energy generated by 2020 (ST, 2015). Nonetheless, RE will still take on the complementary role to fossil fuels due to factors such as output intermittency, location and technology advancement.

Despite incredibly high rates of growth, renewable energy is still only a relatively small part of the global energy picture today. Therefore, this study scrutinized the potential of biochar (biomass) in order to sustain the natural resources.

2.2.1 Biomass Energy

Biomass is regarded as one of the renewable energy sources with the highest potential to contribute to modern society's energy needs for industrialized and developing countries alike. Biomass energy is a fundamental source of energy in most Asian countries, where it exists from living or living organisms. It includes woods, logging wastes and sawdust, animal dung and vegetable matter consisting of leave, crop residues and agricultural waste (Tripathi et al., 2016).

It is an environmentally friendly source and Malaysia has a tradition of producing biomass for the production of electricity. Thus, electricity can be generated by biomass burning, which creates most of the same emissions as fossil fuels. Increasing biomass indeed captures CO₂ from the air so that the net contribution of the cycle to global CO₂ levels is zero (BEC, 2015).

The energy potential of a biomass power plant in Perlis, for instance, used rice husk as the main source of fuel and accumulated 10 MW of power to meet 30,000 households requirements.

2.3 Biomass Sources from Oil Palm Plantation

Palm oil is regarded as Malaysia's most important agricultural crop, with the oil palm industry being the fourth largest contributor to Malaysia's Gross National Income (GNI), generating billions of ringgits (AIM, 2015). Palm oil production is linked to a substantial amount of biomass and its disposal of biomass is one of the key challenges (Abdullah et al., 2013).

Palm oil extracted from palm fruits resulted in a large amount of waste in the form of OPEFB shell and fibre. Malaysia now has over 4 million hectares of land for the planting of oil palms. Over 75% of the total area planted is located in just four states, Sabah, Johor, Pahang and Sarawak. The total OPEFB processed was estimated at 75 million tonnes, while the total OPEFB production was estimated at 16.6 million tonnes while about 58 million tons of palm oil mill effluent (POME) were produced in Malaysia every year (BEC, 2015).

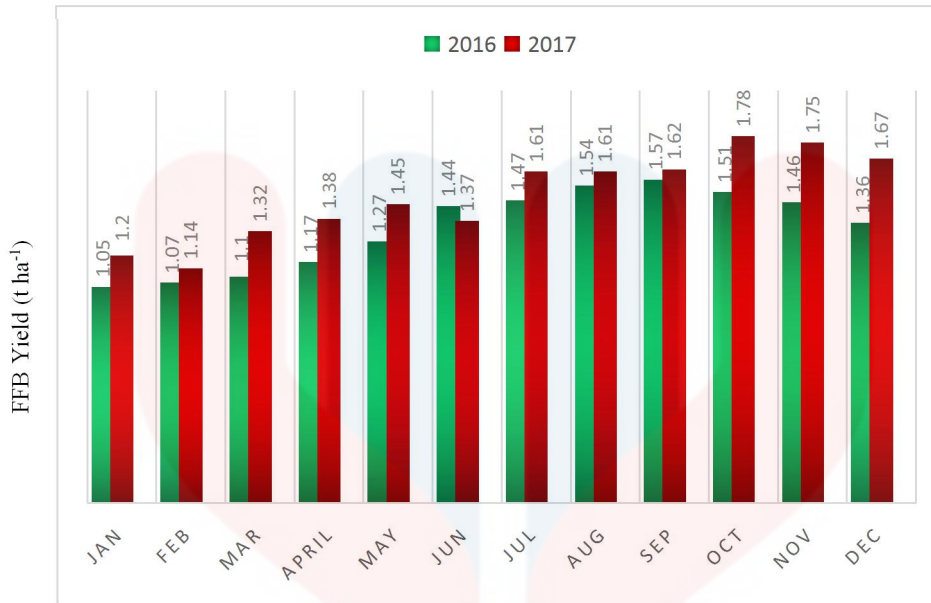


Figure 2.7: Fresh fruit bunches monthly yield in 2016-2017
(Source: MPOB, 2018a)

As mentioned earlier, OPF, OPT, EFB, PKS, MF and POME are produced by six major biomass produced from oil palm industry. According to AIM (2015), oil palm biomass is further classified as solid and liquid waste, making up for a total of 83 million tons of solid waste and 60 million tons of liquid waste generated in 2012. This figure is expected to range from 85 to 110 million tons to 70 to 110 million tons of dry solid and liquid waste by 2020. This projection is consistent with the significant growth of the oil palm planted area in Malaysia.

As stated earlier, most of the biomass is left in the plantations, a situation that demonstrates underutilization of the crucial lignocellulosic feedstock. Approximately 75% of solid waste is OPF and OPT, which are widely available in the plantations, while EFB, MF and PKS, which account for the remaining 25%, are usually available in the mills (AIM, 2015).

2.3.1 Oil Palm in Malaysia

The palm oil industry of Malaysia showed stirring performance in 2017. The output of crude palm oil (CPO) and fresh fruit bunch (FFB) showed statistically significant increases following a year earlier recovery from the impacts of the El-Nino phenomenon (Kushairi et al., 2018).

According to the Department of Statistics, Malaysia, higher palm oil prices and improved export demand led to a dramatic increase in export earnings of RM7,785 billion from RM6,792 billion in 2016. In 2017, the oil palm area planted managed to reach 5.81 million hectares, an increase of 1.3% compared to the previous year's 5.74 million hectares. Sarawak overtook Sabah as the largest oil palm planted state, with 1.56 million hectares or 26.8% of the total Malaysian oil palm planted area, followed by Sabah with 1.55 million hectares or 26.6% and Peninsular Malaysia with 2.7 million hectares or 46.6%. In 2017, CPO production increased by 15%, reaching 19.92 million tonnes as against 17.32 million tonnes in 2016. The increase was due to higher FFB processed, up by 17.7% arising from higher FFB production that increased by 12.4%. CPO production in Peninsular Malaysia, Sabah and Sarawak increased by 19, 7.6 and 15.1% to 10.58, 5.22 and 4.13 million tonnes, respectively.

Table 2.2: Distribution of oil palm planted area by category in Malaysia 2017

Category	Hectarage	
	ha	%
Private estates	3 543 429	61.0
Government schemes	940 326	16.1
Independent smallholders	979 758	16.9
Total	5 811 145	100

(Source: MPOB, 2018b)

In 2017, FFB yield improved substantially by 12.4% to 17.89 tons per hectare, compared with 15.91 tons per hectare in 2016 resulting the distribution of the oil palm

planted area increased in 2017 as stated in Table 2.2. Peninsular Malaysia's FFB yield increased 18.6% to 18.70 tons per hectare compared to 15.77 tons per hectare in 2016. Sabah's FFB yield increased somewhat from 7.3% to 18.35 tons per hectare compared to 17.10 tons, while Sarawak's yield increased equally to 16.13 tons per hectare, up 8.5% from 14.86 tons per hectare in 2016 (MPOB, 2018b).

2.4 Thermochemical Energy Conversion

There are so many advantages embedded in biomass, but before these benefits can be fully exploited, certain pretreatments must be applied to biomass. Chemical, physical, thermochemical and biochemical conversions are the various technologies available to convert oil palm biomass to value added products such as biomass energy. For example, thermochemical is used in this study to produce biochar. The thermochemical conversion process can transfer a wide range of biomass into energy.

This means that biomass is converted into a range of important compounds by a combination of thermal decline and chemical reform. It is achieved either by heating the biomass at different concentrations in the presence of oxygen or by heating it without oxygen (Onnoja et al., 2018a). One of the privileges of this mechanism is that almost all oil palm biomass organic components can be transformed into useful products such as gaseous and liquid fuels. Pyrolysis, combustion, gasification and liquefaction or hydrothermal upgrading are the thermochemical processes (McKendry, 2012).

The conversion process from biomass to energy can be carried out using a variety of different processes and the favoured process is determined by the end user requirements and the sources of the biomass nature. Thermochemical process

included, combustion, gasification, pyrolysis (Cheng, 2014). However, pyrolysis can be made up of two mechanisms where it can be carried out either very slowly or quickly, which defined the pyrolysis type. Conventional or slow pyrolysis in which it has been used for the production of charcoal for millennia, in which biomass is heated for approximately 500°C in about 30 minutes. While mild pyrolysis or torrefaction is the process in which the biomass is heated at a lower temperature especially when compared to the conventional temperature between 200 and 300°C.

2.5 Torrefaction Process

Torrefaction is an attractive proposition to upgrade biomass to a product that retains approximately 90% of its energy. The goal of torrefaction is to improve biomass energy properties. Important advantages of torrefied biomass also include high energy efficiency and hydrophobicity so that moisture does not regain during storage, less smoke when burnt, and a non-fermentable nature (Nithitron & Suthum, 2011). Products that can be used directly as energy or as a chemical feedstock are obtained through these processes. These processes consist of thermal degradation of biomass without oxygen. Of these three products, gas, liquid and solid are commonly obtained in proportions depending on the method used and the operating parameter.

Torrefaction is a thermochemical treatment method with an operating temperature of between 200 to 300°C. It is performed at near atmospheric pressure without oxygen and is characterized by low particle heating rates below 50°C. During the process, biomass partially decomposes with water and various types of volatiles, resulting in a loss of mass and chemical energy in the gas phase. During the process,

two different mechanisms occurred, first during drying, when moisture evaporates and secondly during biomass decomposition.

In the initial heating stage, the evaporation of the biomass moisture content is very slow. The biomass temperature nevertheless increases. The humidity content decreases dramatically in the predrying stage while the biomass temperature remains constant. After this phase, post-drying and intermediate heating takes place. The temperature increases to 200°C and water is released physically.

Above 200°C the torrefaction reaction occurs and in this stage the devolatilization causes the loss of mass. In this condition, where the temperature ranges from 200 to 300°C, humidity in biomass is believed to be vaporized and most volatiles released are from hemicellulose degradation, as hemicelluloses are most reactive in this temperature range and are subject to extensive devolatilization and carbonisation.

In the meantime, other components such as lignin and cellulose are subject to limited devolatilization and carbonisation. This results in a product that characterizes the original raw biomass from the biochar.

2.6 Response Surface Methodology

Response surface methodology (RSM) is a group of math and statistical techniques. One of the main goals of RSM is to determine the optimum control variables settings, resulting in a maximum or minimum response over a certain region of interest. This requires a 'good' fitting model that adequately represents the mean response, since such a model should be used to determine the value of the optimum.

The optimization techniques used in RSM depend on the type of model being installed. The most steep ascent or descent method for first degree models is a viable technique for moving sequentially towards the optimum response. In a multi-response experiment, measurements are obtained on several responses for each setting of the control variables group. There are numerous examples of multi-response experiments, for example a chemical engineer might want to maximize yield while minimizing the cost of a certain chemical process 4 (Andre et al., 2010).

2.7 Optimization and Properties of Torrefied OPEFB Biochar

Analysis procedures were carried out on the torrefied OPEFB biochar by previous study to calculate the yield percentage of biochar products. Proximate analysis was performed to determine the moisture content, volatile matter, ash content and fixed carbon content of torrefied OPEFB biochar. The temperature ranges and heating period for this study were modified with the intention to apply the biochar into soil rather than use it in the thermal energy furnace. The properties of raw and the proximate properties of torrefied OPEFB biochar first involved determining the moisture content were shown in Table 2.3 and Table 2.4, respectively.

Table 2.3: Properties of raw OPEFB

Proximate Analysis (mf wt%)		Ultimate Analysis (%)		Heating Value (MJ kg ⁻¹)	
Moisture content	1.33	Carbon	47.14	HHV	20.61
Volatile matter	77.46	Hydrogen	6.03	LHV	20.34
Ash content	5.29	Nitrogen	<0.1		
Fixed carbon	17.25	Sulfur	0.84		
		Oxygen	45.99		

(Source: Rahman et al., 2014)

According to Table 2.3 shows the raw OPEFB properties from previous study. It can be observed from close analysis that OPEFB feedstock contains a large percentage of volatile matter, 77.46 mf wt% a moderate percentage of ash, 5.29 mf wt% and a small percentage of fixed carbon, 17.25 mf wt%. Due to its high volatile content, OPEFB is suitable for slow pyrolysis. The low percentage of nitrogen and sulphur in OPEFB obtained from the results of the elementary analysis, which is less than 1%, indicates this feedstock's environmentally friendly behaviour (Adilah et al., 2014).

Table 2.4: Proximate analysis results of OPEFB biochar

Biochar	Ash content (mf wt%)	Proximate Analysis (mf wt %)			
		Moisture Content	Volatile Matter	Ash Content	Fixed Carbon
1	5.29	5.15	7.20	19.86	72.94
2	4.65	2.42	6.68	16.53	76.79
3	3.28	2.05	5.46	13.75	80.79
4	2.21	1.15	4.81	10.16	85.03
5	1.60	1.07	4.11	7.55	88.34

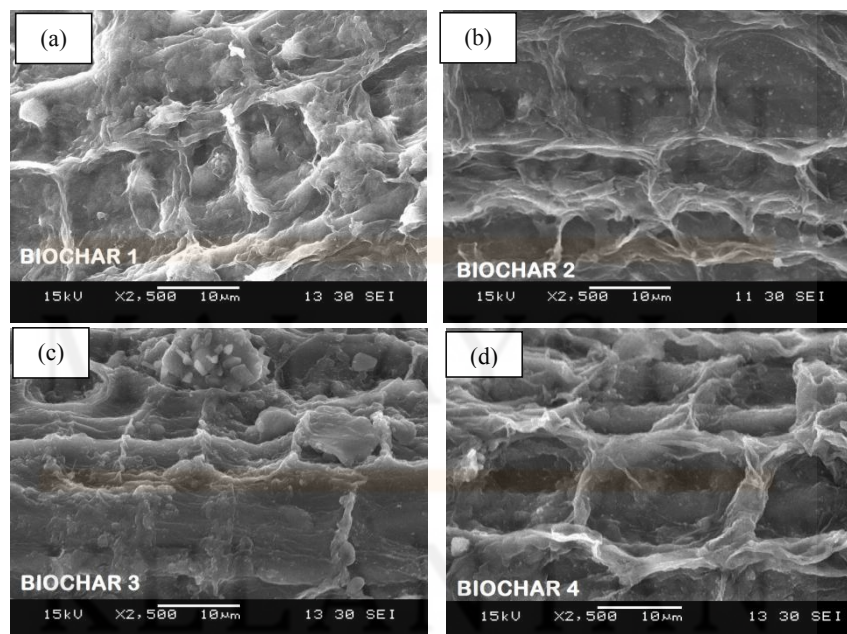
(Source: Rahman et al., 2014)

The results of the proximate properties of biochar are also presented in moisture-free weight percentage, mf wt%. According to the proximate properties results for biochar shown in Table 2.5, it can be observed that as the ash content of EFB feedstock decreased from 5.29 to 1.60 mf wt%, the biochar moisture content decreased from 5.15 to 1.07 mf wt%. The volatile matter of biochar also decreased from 7.20 to 4.11 mf wt%. The ash content of the biochar produced also experienced a decrease from 19.86 to 7.55 mf wt \%. In addition, the fixed carbons in the biochar increased from 72.94 to 88.34 mf wt%. The percentage of biochar carbons determined by elemental analysis also increased as the ash content of the EFB feedstock decreased. The fixed carbon obtained by proximate analysis differed from that obtained by elemental analysis. The fixed carbons in proximate analysis do not

include the carbons in the volatile matter. In addition, a fixed carbon is one of the important elements that determine the quality of biochar as a soil amendment. Good biochar should have a high fixed carbon content.

2.8 Morphological Characterization

A surface morphology study was performed on the OPEFB biochar to observe the effects of various OPEFB feedstock ash contents on the physical characteristics of OPEFB biochar from previous study. According to Adilah et al., (2014) SEM analysis was performed to observe structural changes in OPEFB biochar. High-resolution images of OPEFB biochar were obtained using a JEOL JSM 6400 LV model scanning electron microscope, which was operated at 15 kV. A Quantachrome Autosorb-1 Surface Analyzer was used to determine the BET surface area of the OPEFB biochar.



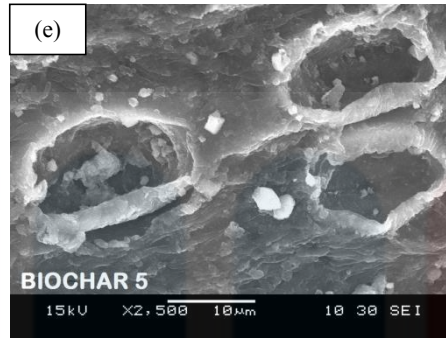


Figure 2.8: SEM images (a, b, c, d and e) of OPEFB biochar with magnification of x2500 (Source: Adilah et al., 2014)

SEM images of biochars produced by EFB feedstock with various ash contents are shown in Figure 2.8. All of the images were magnified 2,500 times. In Figure 2.8(a) it can be observed that the morphological structure of biochar produced from unwashed feedstock is denser and lumpy compared with biochar produced from washed feedstock (Figure 2.8(b)). In Figure 2.8(e), cell wall breakdown can be clearly observed for biochar produced from the lowest ash content (1.6 mf wt %).

2.9 Bonding Behaviour Characterization

FT-IR spectroscopy is a powerful tool for the study of polysaccharide ' physicochemical and conformation properties. Peaks at 1,044 and 3,419 cm^{-1} corresponding to C-O and O-H groups, respectively, are present in OPEFB and OPF fibers. According to (Khalil et al., 2008), the existence of O-H groups is due to the moisture content. The hydroxyl group is found in cellulose, hemicelluloses, and lignin. The prominent peaks at 1,739 cm^{-1} and 1,732 cm^{-1} represent carbonyl stretching (C=O) for acetyl groups in hemicelluloses and carbonyl aldehyde in lignin, respectively. A previous study reported that a peak at 1,378 cm^{-1} indicates the presence of C=O stretching frequency of the carboxylic group in hemicelluloses.

Intense peaks at about 882 cm^{-1} and 1507 cm^{-1} indicates the stretching of the aromatic group such as in lignin.

From previous study also shows the differences in chemical composition between the various types of oil palm fibers. Extractive content was highest in OPT fiber (5.35%) compared to other fibers. This result was in the agreement with the results of a previous study, even though the value of the extractive content obtained is higher (9.8%). OPT fiber is also believed to have a high dimensional stability because its high extractive content (especially oil and wax) will reduce the hygroscopic fiber property. The utilization of OPT fiber in paper production will also reduce the pulp yield. This is because most extractive have a bad impact on chemical and mechanical pulping.

Table 2.5: Chemical composition of oil palm

	Extractive (%)	Holocellulose (%)	Cellulose (%)	Lignin (%)	Ash (%)
EFB	3.21	80.09	50.49	17.84	3.4
OPF	4.40	83.54	56.03	20.48	2.3
OPT	5.35	73.06	41.02	24.51	2.2

(Source: Khalil et al., 2008)

Chemical analysis of oil palm fibers shows that the principal component is cellulose. OPF fiber contains the highest percentage of holocellulose (83.54%) and α -cellulose content (56.03%) stated in Table 2.5. Similar results were obtained in previous studies. They reported that the content of α -cellulose in OPT waste was slightly low (29.2–41%). The amount of cellulose in fibers will affect the property

and economic production of fibers for various uses. In pulp and paper technology, the strength of paper depends on the content of cellulose in the natural plant.

Generally, OPT fiber showed the highest percentage of lignin (24.51%), followed by OPF (20.48%) and EFB (17.84%). This was expected since mature tissues at the base (trunk) accumulate higher amounts of metabolic products than the younger parts at the top (frond and branches). Lignin is a desirable polymer and its removal during pulping requires high amounts of energy and chemicals. EFB fibers had the lowest lignin content, which indicates that this material can undergo bleaching more easily and with the utilization of fewer chemicals than OPT fibers (Khalil et al., 2008).

2.9.1 Characteristic IR Absorption Frequencies of Organic Functional Groups

A molecular spectroscopy which used to characterize both organic and inorganic evidence. The sample is bombarded with infrared radiation then the frequency of infrared radiation will match the natural frequency of the bond. Thus, the amplitude of the vibration will increase and the infrared will be absorbed. Table 2.6 shows the characteristic IR absorption frequencies of some organic functional groups.

Table 2.6: IR Absorption Frequencies of Organic Functional Groups
(Source: (Isroi et al., 2012))

Functional Group	Type of Vibration	Characteristic Absorptions (cm ⁻¹)	Intensity
Alcohol			
O-H	(stretch, H-bonded)	3200-3600	strong, broad
O-H	(stretch, free)	3500-3700	strong, sharp
C-O	(stretch)	1050-1150	strong
Alkane			
C-H	stretch	2850-3000	strong
-C-H	bending	1350-1480	variable

Alkene			
=C-H	stretch	3010-3100	medium
=C-H	bending	675-1000	strong
C=C	stretch	1620-1680	variable
Alkyl Halide			
C-F	stretch	1000-1400	strong
C-Cl	stretch	600-800	strong
C-Br	stretch	500-600	strong
C-I	stretch	500	strong
Alkyne			
C-H	stretch	3300	strong, sharp
			variable, not present in symmetrical alkynes
-C≡C-	stretch	2100-2260	
Amine			
N-H	stretch	3300-3500	medium (primary amines have two bands; secondary have one band, often very weak)
C-N	stretch	1080-1360	medium-weak
N-H	bending	1600	medium
Aromatic			
C-H	stretch	3000-3100	medium
C=C	stretch	1400-1600	medium-weak, multiple bands
Analysis of C-H out-of-plane bending can often distinguish substitution patterns			
Carbonyl			
C=O	stretch	1670-1820	strong
(conjugation moves absorptions to lower wave numbers)			
Ether			
C-O	stretch	1000-1300 (1070-1150)	strong
Nitrile			
CN	stretch	2210-2260	medium
Nitro			
N-O	stretch	1515-1560 & 1345-1385	strong, two bands

CHAPTER 3

MATERIALS AND METHODS

3.1 Materials

Material that being used in this study was OPEFB fibre (Figure 3.1) which is derived from fibre mill at Penang. OPEFB was selected due to its potential as renewable biomass source since it was locally abundant in Malaysia.

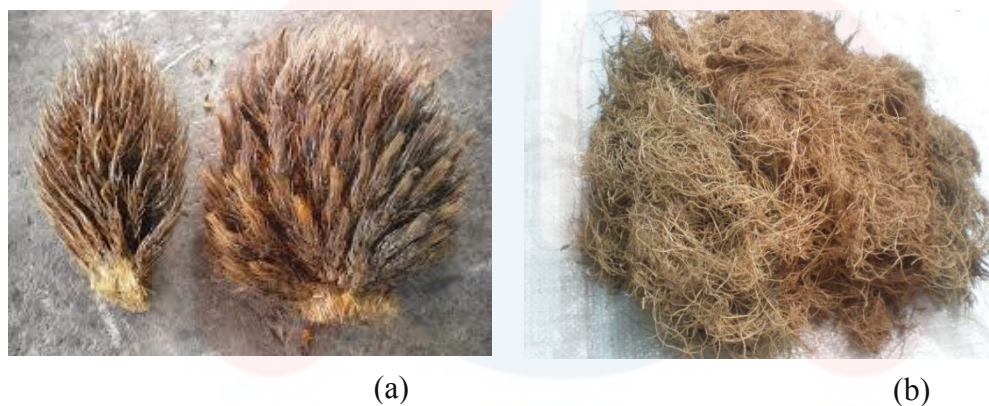


Figure 3.1: (a) Raw OPEFB and (b) OPEFB fibre used for torrefaction

3.1.1 Sample Preparation

The raw OPEFB which is contained lignocelluloses, oil and water was soaked into fresh water to make it became thoroughly wet for a certain period in order to remove the residual oil. Then, it was teared apart to lose the fibrous strands, which was washed with tap water, cleaned, sorted and dried for 24 hours under the direct sunlight to get it dry. It was then oven-dried at constant temperature at 103 ± 2 °C for 1 hour to minimize the moisture. The OPEFB fiber was cut into length of

approximately 3mm length in order to get a better quality fiber before further treatment.

Next, the dried OPEFB fibre was grinding before undergo next process. Then, it was screening into three different sizes which is 250, 500 and 750 μ m. The purpose of grinding and screening the OPEFB fibre was to obtain a desired sample scales without any contamination of unwanted particles such as dust that might affect the final results when the sample being analyzed. Figure 3.2 showed the overall process from material, sample preparation, methods and analysis for this study.

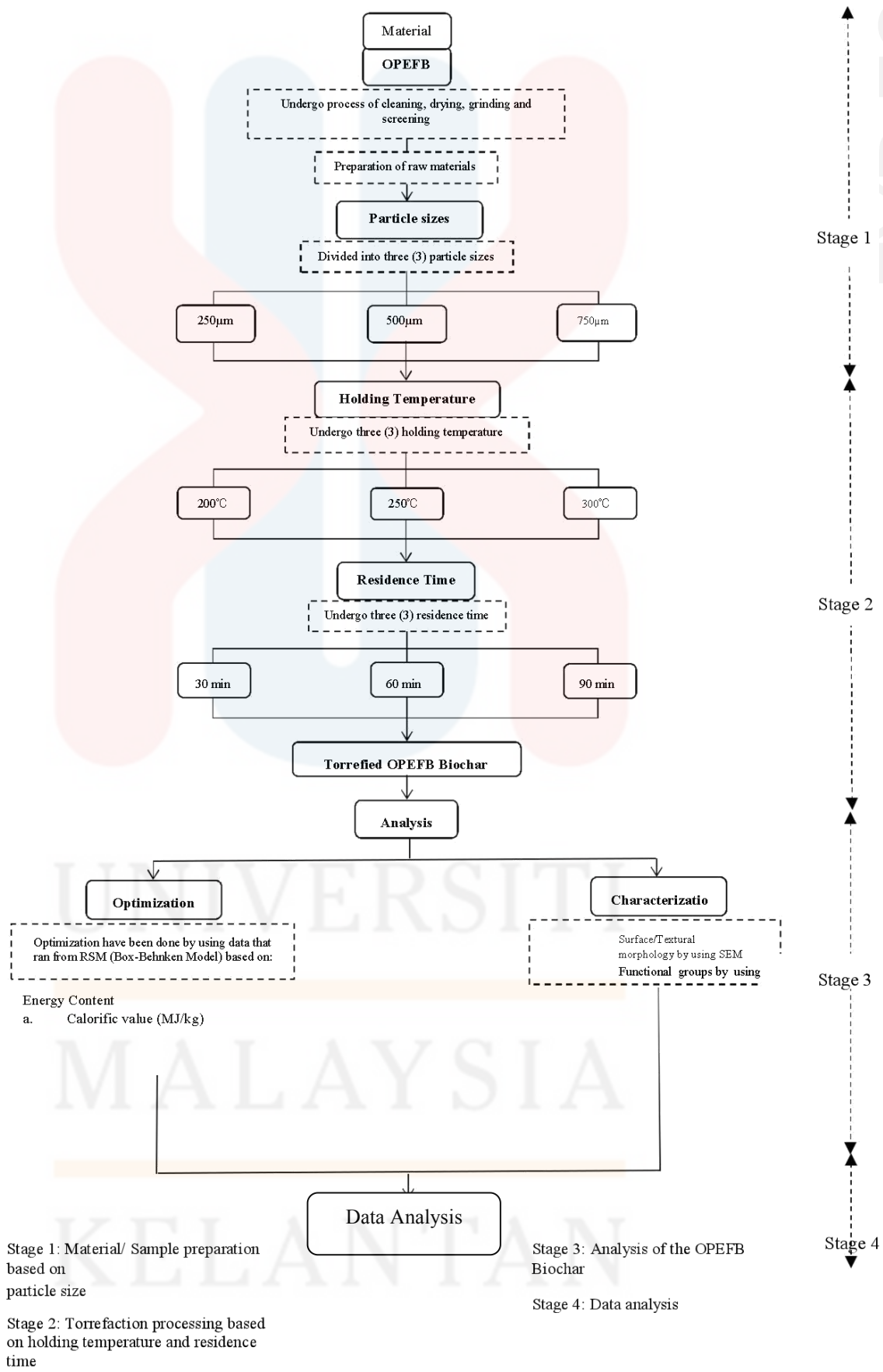


Figure 3.2: The overall process of torrefied OPEFB biochar

3.2 Methods

Process that involved in this study was divided into four stages which is started with the sample preparation based on particle size, torrefaction processing based on their holding temperature and residence time, the analysis of the torrefied OPEFB biochar and last but not least the data analysis.

3.2.1 Torrefaction Process

In this study, the OPEFB fibre was undergone thermal pretreatment method as mention in Section 2.5, known as torrefaction process before being analyzed. The process was taken places within three holding temperatures varied at 200, 250 and 300°C in the absence of O₂ under a low heating rate by using furnace also with three residence time within 30, 60 and 90 minutes. The heating rate was recorded every minute according to the residence time during the burning phase. The product of this torrefaction process then was known as torrefied biochar.

3.2.2 Optimization

In order to get the optimization, a statistical technique, RSM (Box-Behnken model) was used to aid in these process. It was purposely used to optimize a response which influenced by several independent variables as stated in Section 1.4. The optimization have been done by using data that running by RSM based on energy content (calorific value).

i. Mass Yield

The mass yield (M_Y) of the torrefaction process was the actual mass of the torrefied OPEFB biochar obtained. So, in this study the percentage yield can be calculated as the final (theoretical) mass of the product with the initial mass of product, giving the percentage figure for the reaction. The percentage of the M_Y in this process was worked out from the Equation (3.1) as followed:

$$MY = \frac{\text{Weight of mass after torrefaction}}{\text{Mass of raw OPEFB}} \times 100 \quad (3.1)$$

ii. Proximate Analysis

Proximate analysis was used in this study to determine the moisture content, volatile matter, ash content and fixed carbon. It was the evaluation of the yield of various products obtained upon heating under controlled conditions and important in identifying the optimization of any thermochemical conversion process (Cheng, 2014).

a. Moisture Content

In order to get the moisture content (MC), moisture analyzer MX-50 was used according to ASTM D3173. The torrefied OPEFB biochar was put on the pan support properly and weighed. The heating cap was closed and the analysis was started. The machine was lit indicated the analysis of the sample was started. Thus, the reading

was recorded after the signal sound was produced by the equipment. Equation (3.2) was used for MC calculation:

$$MC = \frac{(W_i - W_f)}{W_f} \times 100 \quad (3.2)$$

Where, W_i = Initial weight and W_f = Final weight

b. Volatile Matter

To analyse the volatile matter (VM), it had been done by using furnace according to ASTM D3173. According to the standard procedures, the crucible without the cap was weighed by using the analytical balance and 1.00 g of the sample was put into the crucible and weighed. Then the crucible with the samples together with its cap was weighed and the weight was recorded. By the time, the furnace was preheated to 900 °C and the top of the crucible was covered using a cap. It was burnt in 900°C for 7 minutes and the samples were taken out from furnace and weighed when it done. The following Equation (3.3) was used to determine the VM:

$$VM = \frac{W_i - W_f}{W_i} \times 100 \quad (3.3)$$

Where, W_i = Initial weight and W_f = Final weight

c. Ash Content

As for analysing the ash content (AC), according to ASTM D3173 it still was done by using furnace. The furnace was preheated to 815°C previous testing were put into the furnace without its cap. Then the cap on the top of the crucible was withdrawn. All the crucibles without the cap were then put into the furnace and burnt in 815 °C for three hours. After the samples were taken out from the furnace, it was weighed and recorded. Equation (3.4) was used to calculate the AC as followed:

$$AC = \frac{\text{Weight of residue}}{W_f} \times 100 \quad (3.4)$$

Where, W_f = Final weight

d. Fixed Carbon

After the reading of MC, VM and AC of the samples that were obtained, the fixed carbon (FC) was calculated by using 100% deduct the percentage of moisture content, volatile matter and ash content of each samples. The formula was as Equation (3.5) as followed:

$$FC = 100\% - (MC\% + AC\% + VM\%) \quad (3.5)$$

ii. Energy Content

The calorific value (CV) of a material was an expression of the energy content, or heat value, released when burnt in air. It measured in terms of the energy content per unit mass, or volume; hence MJ/kg for solids, MJ/l for liquids, or MJ/Nm³ for gases. In order to analyse the CV, auto calorimeter 500 according to ASTM D2015 were done in this study. The auto calorimeter 500 and its paired computer were switched on one hour before the analysing. The combustion chamber was ensured to be in dried condition and the O₂ gas valve was opened. The sample was weighed to more than 1g and the name and weighed of the sample were put into the computer. Then, the holder crucible was placed in the workstation and put into it. The ignition wire (2-3cm) was then coiled in U- shaped and tied to both end connectors above the crucible. The cap vessel was closed and tightened and the O₂ was put into it. Distilled water was put into the bucket and then placed into the chamber. The wire was connected to the connector on the bucket. The 'F5' button was clicked on the computer to start the analysis and equilibrating was carried out around 3-7 minutes.

3.2.3 Characterization Analysis

The potential roles of torrefied biochar were all largely depended on the surface properties of the biochar (Ok et al., 2016). From previous study, there have been multiple studies analyzing surficial physical and chemical properties of the torrefied biochar to optimize the potential mechanisms. So, in this study the torrefied OPEFB biochar undergone characteristic analysis in terms of the surface morphology and its bonding behaviour.

To analyse both characteristics of the torrefied biochar, SEM and FTIR were used in this study. The morphology characteristics were obtained as an image measured by the size, shape and the structure of the torrefied OPEFB biochar.

As part of this characterization, the bonding behaviour was examined to obtain information on the molecular bonds and the functional group content in the torrefied OPEFB biochar were identified. In this study, the range of IR region have been measured in term of the wave numbers between 4000-500 cm^{-2} . The background IR emission spectrum was recorded, followed by IR source emission spectrum with torrefied OPEFB biochar.

Nevertheless, the same analysis were conducted for both raw and torrefied OPEFB biochar and had been discussed detail in Section 4.7.

3.3 Data Analysis

Last but not least, the raw and torrefied biochar of OPEFB have been analysed, evaluated as well as compared between the surface morphology and the bonding behaviour based on data obtained. All the data were analyzed by using ANOVA.

CHAPTER 4

RESULTS AND DISCUSSION

4.1 Physical Appearance of Raw and Torrefied OPEFB Biochar

Figure 4.1 shows the solid products for the torrefaction process which is the torrefied OPEFB biochar while Figure 4.1(a) is the raw OPEFB fiber. The colour variation of the torrefied biomass products depend on the torrefaction parameters such as holding temperature and residence time (Thuraiya, 2016; Thuraiya and Ruwaida, 2016). As the residence time increases, the intensity of the torrefied OPEFB biochar colour became darker as shown in Figure 4.1.

Based on the figures shown, it presented the sample of raw and torrefied OPEFB biochar at different holding temperature and residence time. Figure 4.1(b), (e) and (h) are the sample of torrefied OPEFB biochar in 30 minutes, Figure 4.1(c), (f) and (i) are the sample of torrefied OPEFB biochar in 60 minutes while Figure 4.1(d), (g) and (j) are the sample of torrefied OPEFB biochar in 90 minutes, respectively.

It shows that the colour of the torrefied biomass changed from light brown to black as the holding temperature increased. At 200°C, the colour of the torrefied OPEFB biochar is slightly brownish in colour which is indicated that at 200°C, the biochar was not completely burnt. In contrast, at 300°C, the colour of the biomass was completely pure black. According to Tumulu et al. (2011), the colour changes may be due to drying process took place during torrefaction while removing of surface and bound water from the raw biomass and resulted reducing in moisture content.

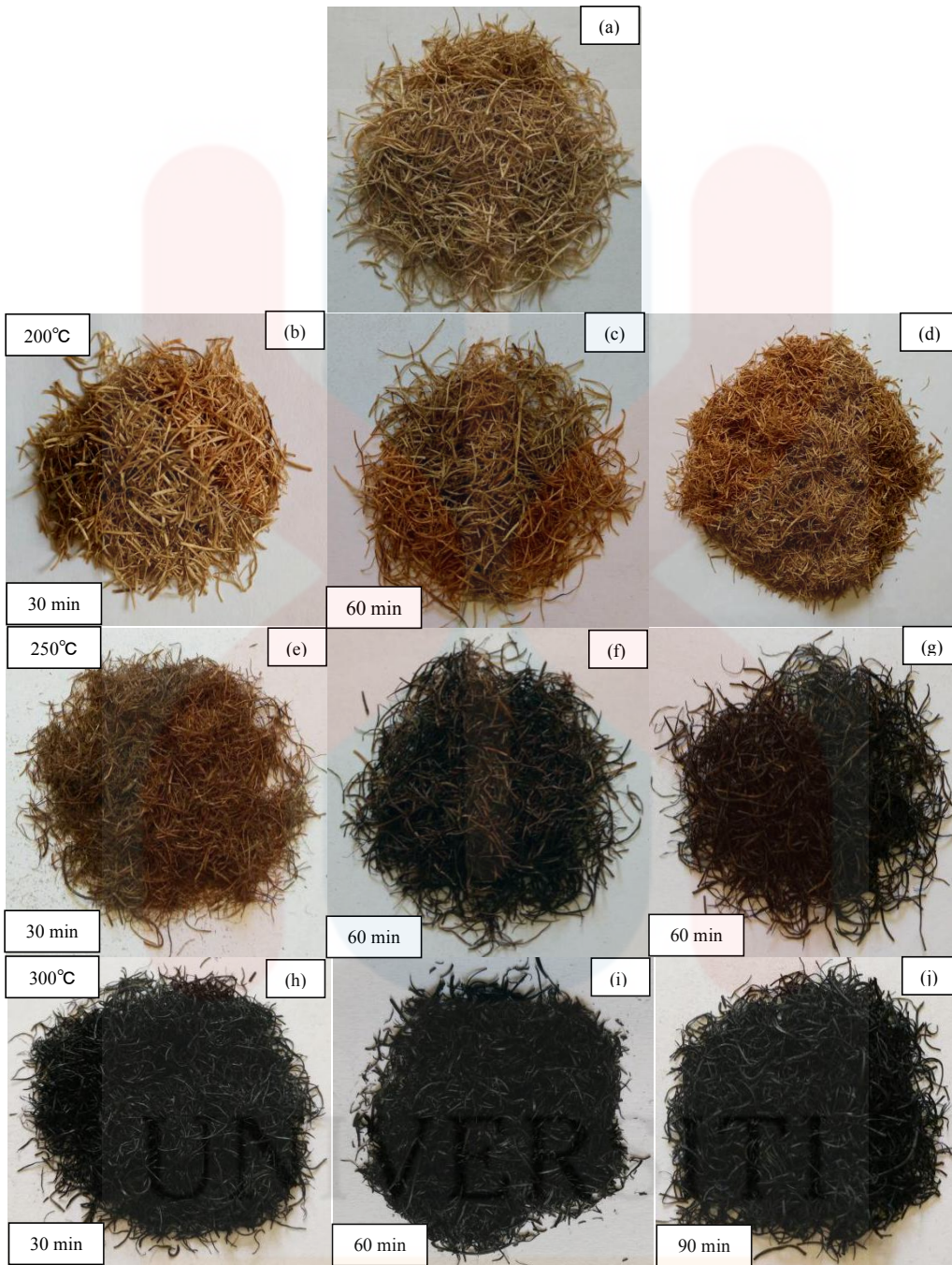


Figure 4.1: Samples of Raw and Torrefied OPEFB Biochar

4.2 Mass Yield of Torrefied OPEFB Biochar

Mass yield at various temperature in 30, 60 and 90 minutes torrefaction residence time shown respectively, in Figure 4.2. The effect of holding temperature and

residence time on the percentage of torrefied OPEFB biochar mass yield can be seen declining as the holding temperature increases from 200 to 300°C.

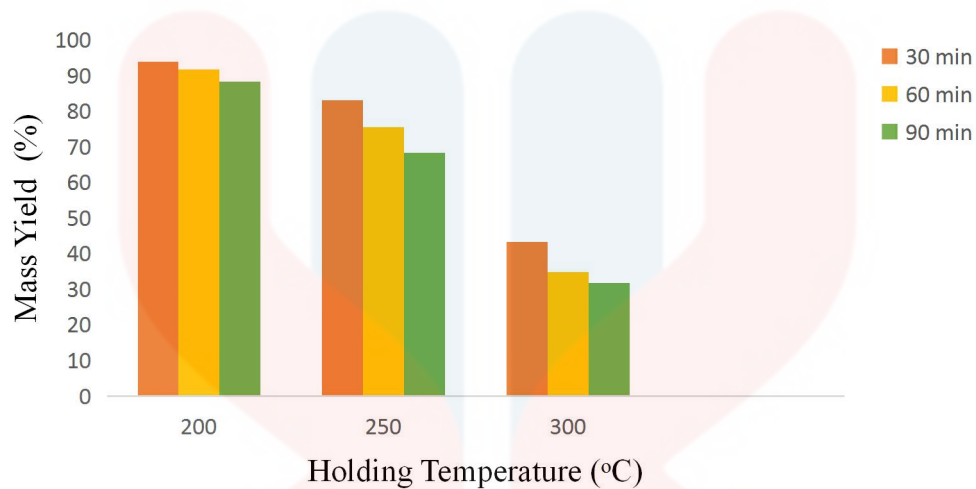


Figure 4.2: Effect of holding temperature and residence time on the mass yield

At 200°C, the percentage of the mass yield decreases from 93.95, 91.77 to 88.25%, at 250°C, the percentage of the mass yield decreases from 83.12, 75.57 to 68.34% and at 300°C, from 43.36, 34.78 to 31.75% as the holding temperature and the residence time increases. It might explain the severity of thermal exposure would lead to extend further the decomposition of the torrefied OPEFB biochar (Iqbal et al., 2016). On the other hand, the mass yields gradually decrease over the range of holding temperature and also the residence time from 30 to 60 min of torrefaction. Increasing the holding temperature increases the heating exposure during torrefaction process, thus results in secondary cracking and depolymerisation occurs between 200 to 300°C for hemicelluloses (Iqbal et. al, 2017).

4.3 Proximate Properties for Raw and Torrefied OPEFB Biochar

Proximate properties for the biochar which is moisture content, volatile matter, ash content and fixed carbon have been done in this study for raw and torrefied OPEFB biochar. The results of the proximate analysis of biochar are also presented in APPENDIX-A (Table A.4).

4.3.1 Moisture Content

Moisture content at various temperature in 30, 60 and 90 minutes torrefaction residence time shown respectively, in Figure 4.3.

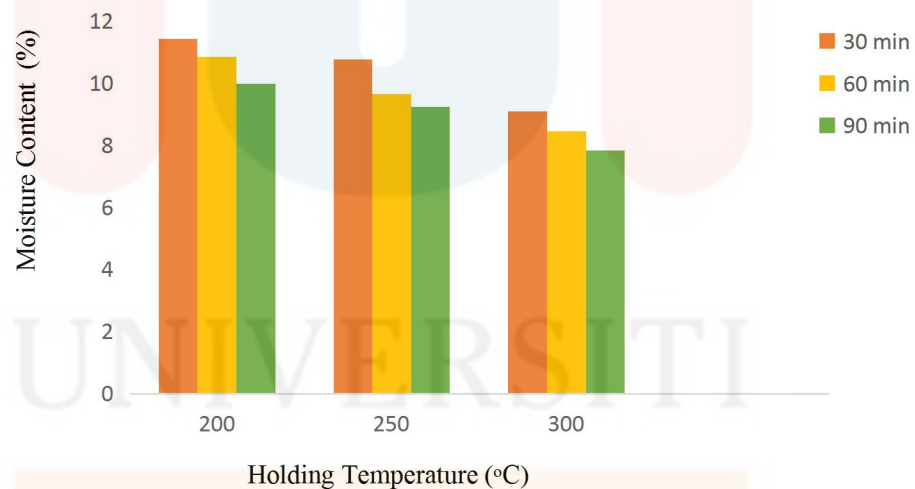


Figure 4.3: Effect of holding temperature and residence time on moisture content

At 200°C, the percentage of moisture content in the torrefied OPEFB biochar slightly fall from 11.43, 10.86 to 9.98% and at 250°C, from 10.76, 9.65 to 9.23% and at 300°C from 9.1, 8.46 to 7.83%, respectively as the residence time increases from 30 to 90 minutes of torrefaction. Based on the result, the effect of holding temperature

and residence time on the percentage moisture content exhibited the lowest at 300°C, 90 minutes of torrefaction reaction where the higher the holding temperature, the lower the moisture content. In thermochemical process, any moisture content in the biochar should be reduced before the first stage of combustion can occur, requiring energy, and thus reducing overall torrefaction process efficiency and potentially reducing combustion temperature below the optimum. Moreover, reduction in combustion temperature below the optimum may result in incomplete combustion of the biochar.

4.3.2 Volatile Matter

Biochar volatile content, or the degree of carbonization, can play a critical role in determining its fuel reactivity.

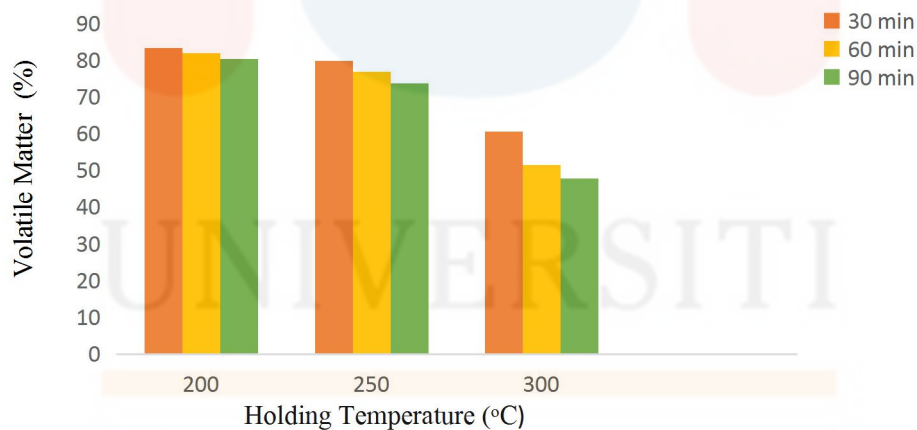


Figure 4.4: Effect of holding temperature and residence time on volatile content

Figure 4.4 show volatile content at various temperature in 30, 60 and 90 minutes torrefaction residence time shown, respectively. The effect of holding temperature and residence time on the volatile percentage percentage of torrefied OPEFB biochar can be seen only a small change changes at 200°C from 83.24, 81.91 to 80.4%. A

gradual change shown at 250°C from 79.81, 76.89 to 73.7% and then fluctuated again at 300°C from 60.62, 51.53 to 47.77%. From the result, generally the percentage of the volatile content portrayed the lowest at at 300°C, 90 minutes. According to Koppejan & Loo, (2012) biomass became highly reactive fuel as the volatile content is high causes a faster combustion rate during the volatilization phase than other fuels such as coal. Moreover Iqbal et al. (2017) stated that biomass typically have more than 80% volatile content higher compared to coal which had lower volatile content which is less than 20%. Therefore, lower volatile content might closer the torrefied biomass to coal.

4.3.3 Ash Content

The percentage of ash content in the torrefied OPEFB biochar at various temperature in 30, 60 and 90 minutes torrefaction residence time shown respectively, in Figure 4.5.

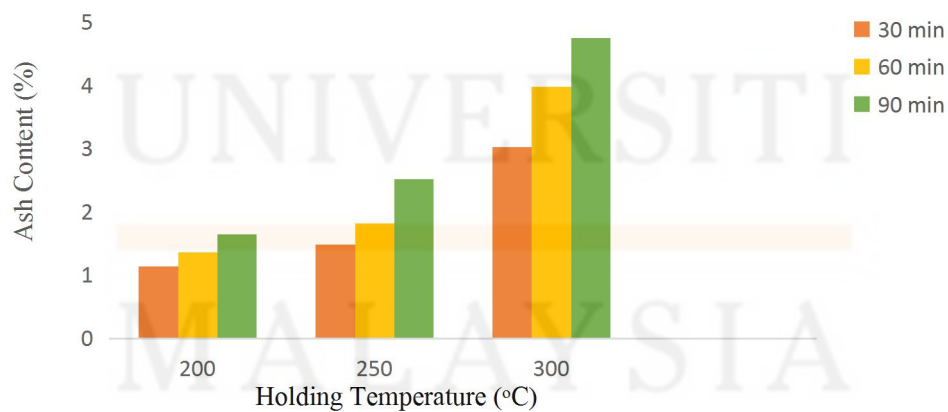


Figure 4.5: Effect of holding temperature and residence time on ash content

Based on the result shown, there is significant changes on the ash content percentage. The percentage shows a rise at 200°C, 1.14, 1.36 to 1.65% of ash content.

As the holding temperature increased to 250°C, the trend displayed a rise on the ash content percentage on the biochar which is from 1.48, 1.82 to 2.52% compared to percentage of ash content at 300°C, the result shows the highest percentage rises from 3.02, 3.98 to 4.75% compared to other holding temperature. Generally, as the holding temperature and residence time for the torrefaction increased, the ash content percentage in the torrefied OPEFB biochar increased. Akowuah (2012), stated that, the combustion volume and efficiency is affected as the ash content in a fuel is high thus, increase dust emissions (Akowuah et al., 2012). It does not contain toxic metals like coal ash but its composition is important to prevent the corrosion. The combustion temperature significantly affects the total yield of ash from biomass.

4.3.4 Fixed Carbon

Figure 4.6 presents the correlation between fixed carbon contained in the torrefied OPEFB biochar against holding temperature at various residence time of torrefaction from 30, 60 and 90 minutes respectively.

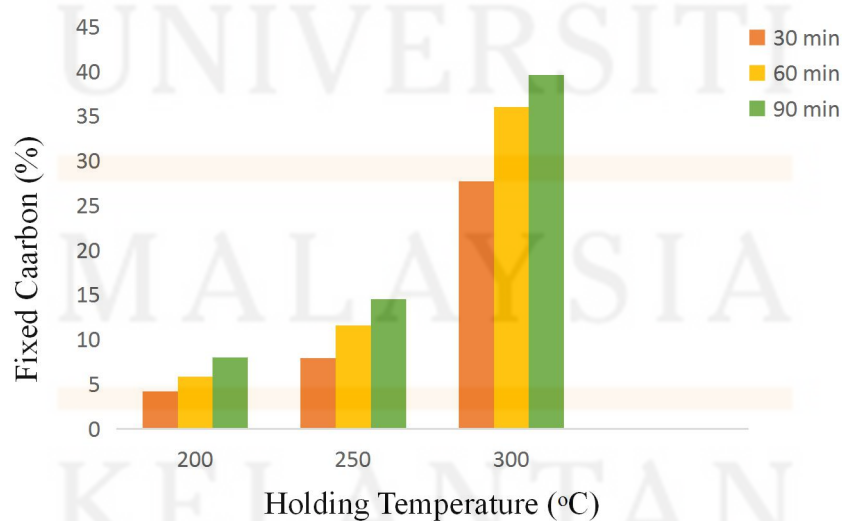


Figure 4.6: Effect of holding temperature and residence time on fixed carbon

The fixed carbon percentage increased from 4.19, 5.87 to 8.03% at 200°C as the residence time of torrefaction increased. At 250°C, the percentage of fixed carbon slightly increase from 7.95, 11.64 to 14.554%. At 300°C, it shows another rise from 27.76, 36.03 to 39.65%. Generally the trend illustrated in Figure 4.6 showing that at 200°C holding temperature was the lowest percentage fixed carbon content in the torrefied OPEFB biochar. According to Dhungana (2011), this is because torrefaction does not removes any component of ash in the biomass but it helped increasing other components of the biochar and along increased their percentage. In addition, a fixed carbon is one of the important elements that determine the quality of biochar where good biochar should have a high fixed carbon content (Adilah et al., 2014).

4.4 Energy Content

The relationship between the calorific value against the holding temperature are shown in Figure 4.7 below on various residence time of torrefaction in 30, 60 and 90 minutes respectively.

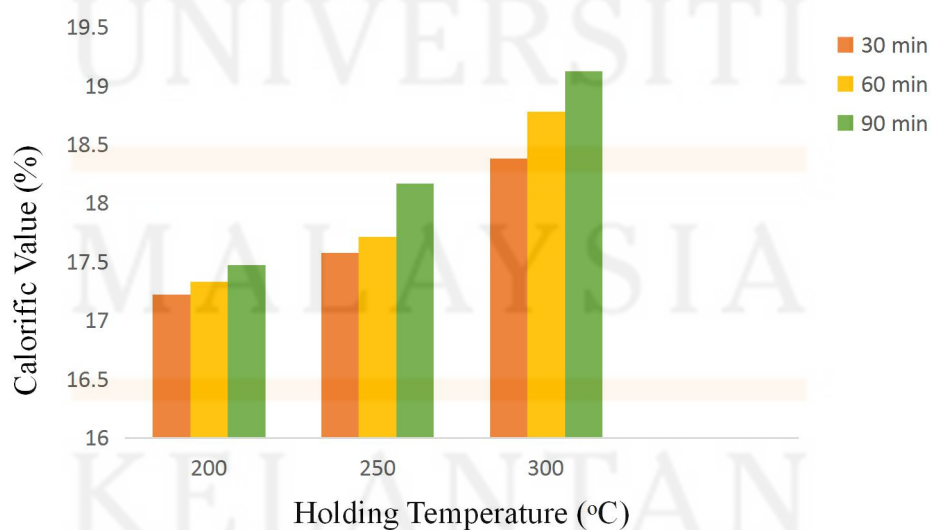


Figure 4.7: Effect of holding temperature and residence time on calorific value

Based on the graph presents, the percentage of CV showing a rise from 17.22, 17.33 to 17.47% at 200°C. At 250°C, the percentage continuously increase from 17.58, 17.71 to 18.17% while at 300°C, the trend shows another rise from 18.38, 18.78 to 19.12%. The percentage of calorific value portrayed the highest at holding temperature of 300°C. It shows that the energy content increased with longer torrefaction reaction time. It is because the increases in carbon content during thermochemical process will affect the oxygen content. It portrayed that increase in calorific value of the torrefied OPEFB biochar at holding temperature 250-300°C in which confirmed to rise in the carbon content.

4.5 Optimization of Raw and Torrefied OPEFB Biochar

Optimization study of the energy content of the torrefied OPEFB biochar using the response surface method (RSM) would ultimately determine the ideal condition for experimental work and the most important independence variables in the experimental process. In addition, this could save time and cost, as the number of experimental works could be reduced

The statistical significance of mean square and P-value was tested using ANOVA from the RSM where the statistical method subdivides the total variation in a set of data into component parts linked with specific source of variation for the purpose of testing hypothesis on the independent variables of the model (Rusly & Ibrahim, 2010). There are few requirements need to take in count for the design model fit which is the F-distribution test, coefficient of determination R and adjusted R² and lack-of-fit test which can be obtained from the ANOVA analysis as referred in APPENDIX-B.

Table 4.1: Analysis of ANOVA for calorific value

Source	Sum of Squares	Mean Square	F Value	P-value
Particle Size	1.596E-005	1	2.718E-004	0.9873 ^{ns}
Holding Temperature	3.57	1	60.84	0.0001 ^{**}
Residence Time	0.42	1	7.20	0.0314 [*]

*significant at 95%, **significant at 99%, ^{ns}not significant

From the ANOVA shown in Table 4.1, P-value less than or equal to 0.05 indicates the model terms are significant. In this case, holding temperature and residence time showed the significant levels at 0.0001 and 0.0314, respectively. However, the values greater than 0.05 indicate the model terms are not significant. There is insignificant model terms identified by RSM on particle size.

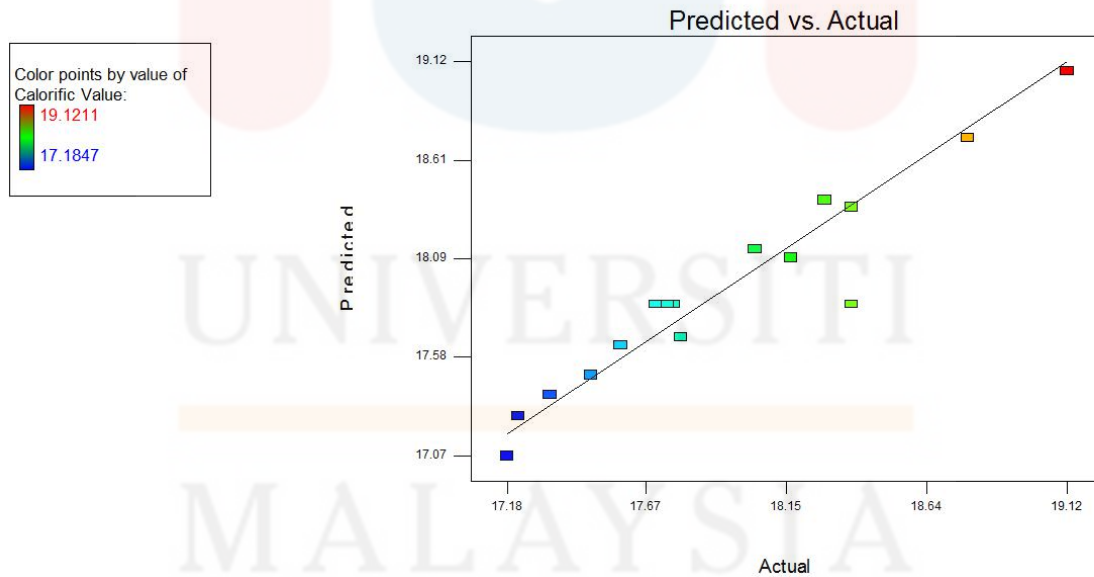


Figure 4.8: Regression between the actual and predicted values for of the torrefied OPEFB biochar optimization on calorific value

Figure 4.8 illustrated the regression between the actual (experimental) and the predicted values for the torrefied OPEFB biochar on the CV where the actual are almost near the predicted values.

The results of analysis of variance (ANOVA) in Table 4.1 revealed that the developed quadratic model was significant for the calorific value predicted under the studied experimental condition. Based on the experimental results acquired, it indicates that the model was significant at 0.01% chance that the model F-value happened due to noise. From the results, holding temperature was the most influential parameter among those 3 independence variables which attained 60.84 of F-value, followed by residence time with 1.76 of F-value. The least influential independence variable was the particle size which scored 2.718E-004 of F-value. Furthermore, the P-value should be < 0.05 to validate the significant of the design model. The value of 0.27 implied that the lack of fit was not significant relative to the pure error. There was 84.54% chance of this lack of fit occurred which was large due to noise. Non-significant lack of fit depicted that the model was good and well fitted in the experiments. Furthermore, referring to ANOVA in Table 4.1, only the interaction between holding temperature and residence time show significant effects on the response since the significant of the design model which is the P-value was set at < 0.05 .

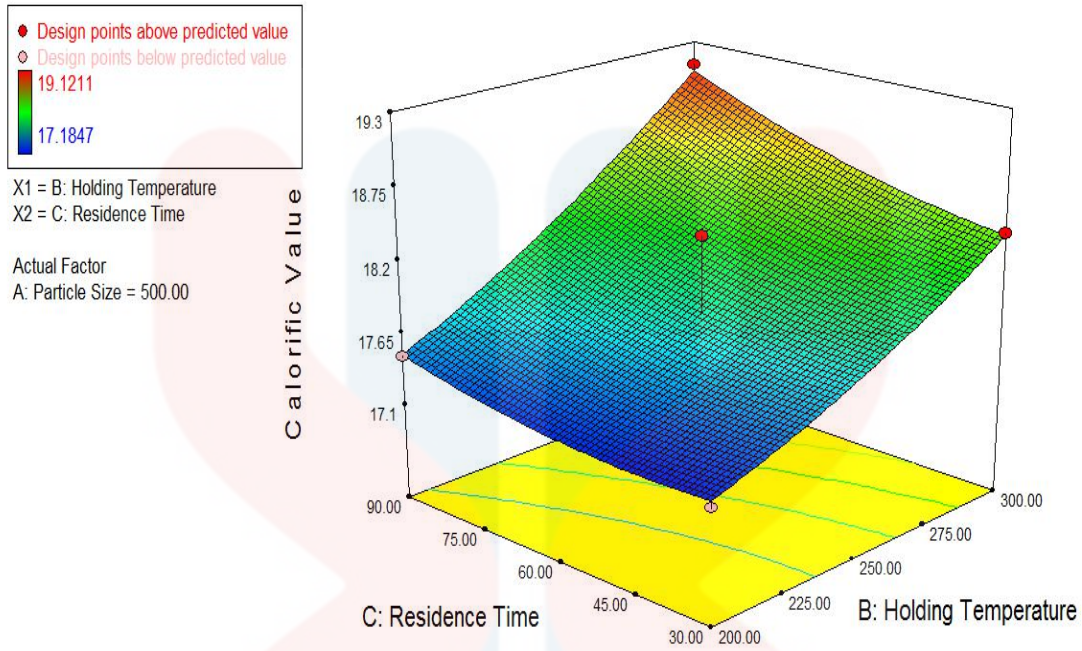


Figure 4.9: Response surface 3D curve of the torrefied OPEFB biochar optimization on its calorific value

As displayed in Figure 4.9, the response 3D surface curve showed the relationship between the holding time and the residence time on the CV of torrefied OPEFB biochar. It was found that increasing the holding temperature from 200 to 300°C along with the residence time from 30 to 90 min of torrefaction, increased the calorific value within those levels. At 300°C holding temperature, the calorific value portrayed the optimal value is in between 17.1847 to 19.1211 MJ/kg on 90 minutes of torrefaction process.

Table 4.2: Optimum condition suggested by RSM

Exp.	Particle Size (µm)	Holding Temperature (°C)	Residence Time (min)	Predicted Calorific Value (MJ/kg)	Actual Calorific Value (MJ/kg)	Deviation (%)
1	500	300	90	19.1393	19.1007	3.12

Validation of the experiment was performed at the optimum conditions as illustrated in Table 4.2 to obtain the most optimized torrefied OPEFB biochar.

Response optimum values were verified from the independence variables which holding temperature and residence time, respectively. The calorific value was estimated as 19.1393MJ/kg within these optimum conditions at 300°C of holding temperature in 90 minutes of residence time while the actual experiment conducted showed the calorific value was 19.1007MK/kg it indicates a very high degree of precision demonstrating the result found is precise. At the same time, the deviation obtained was under 5% (3.12%) showing that the variability response is 95% can be fit by the model. The CV is low indicated that is a very high degree of precision and reliability of research results in this study (Oramahi & Diba, 2013; Sun et al., 2010).

4.6 Morphology Properties of Raw and Torrefied OPEFB Biochar

The analysis of the scanning electron microscopy (SEM) was carried out to view the raw OPEFB fibre morphological structure and torrefied OPEFB biochar. Structure of OPEFB was observed under different magnifications as shown in Figure 4.10 to Figure 4.13 from size, shape, and wall structure cell aspects, OPEFB generally show variety that is high. All of these fibre structures are almost round in shape as shown in the figures.

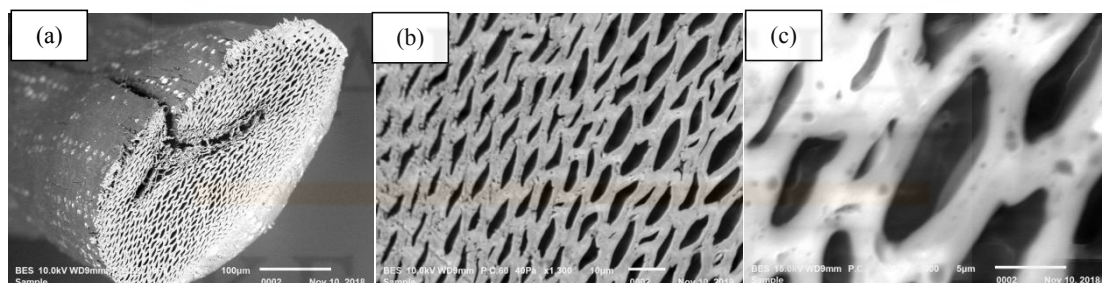


Figure 4.10: SEM images of raw OPEFB surface structure sieved 500µm (a) magnification x250, (b) magnification x1500, (c) magnification x5000

SEM images shown in Figure 4.10 illustrated the surface structure of raw OPEFB fibre with different magnification of x250, x1500 and x5000 respectively. The raw OPEFB fibre had a rigid surface with a matrix layer like lignin or wax covering the entire fibre surface. This layer might be the protective layer in most plants to counter the water loss. From the SEM images observed, the cell walls of this biomass were thicker than hardwood, resulting in a high level of coarseness and rigidity, as previous studies have reported.

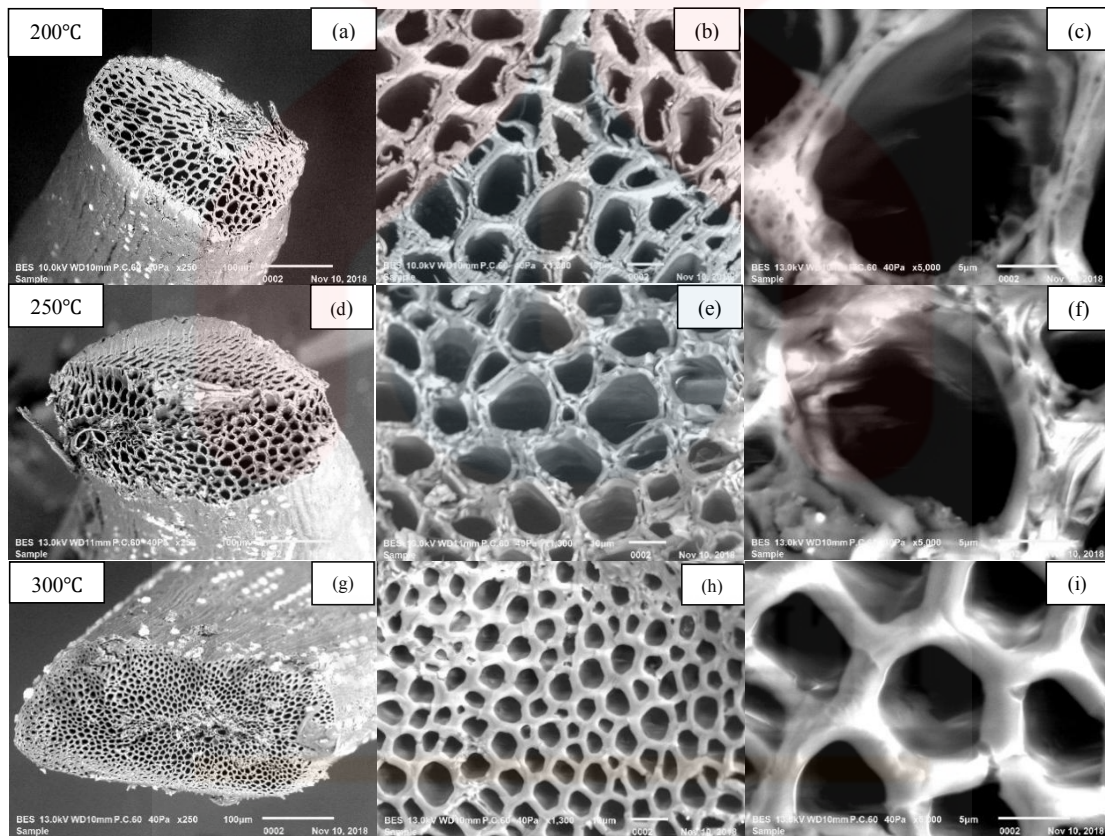


Figure 4.11: SEM images of torrefied OPEFB biochar surface structure on 30 minutes of torrefaction at respective holding temperatures with magnifications of x250 (a, d and g), x1500 (b, e and h) and x5000 (c, f and i)

SEM images shown in Figure 4.11 illustrated the surface structure of torrefied OPEFB biochar with different magnification of x250, x1500 and x5000 respectively for 30 minutes of residence time. The torrefied OPEFB biochar had less rigid surface and some physical changes such as a rough fibre surface can be observed in Figure

4.11(b). Changes in the fibre surface occur due to the treatment process. Another observation revealed from the SEM images of the torrefied OPEFB biochar is the existence of pores on the fibre surface as presented in Figure 4.11(c). The SEM images show that the torrefaction process on OPEFB fibre for the holding temperature of 30 minutes is capable of increasing the porosity. Previous study reported this is because the strand formation is an indication that the structure has been loosened up due to delignification. Since lignin acts as glue and often referred to as the plant cell wall adhesive, thus when delignification process occurred, the bonding between cellulose strands loosened (Ariffin et al., 2008). Hemicellulose removal was also occurred as the pores are clearly seen in Figure 4.11(i).

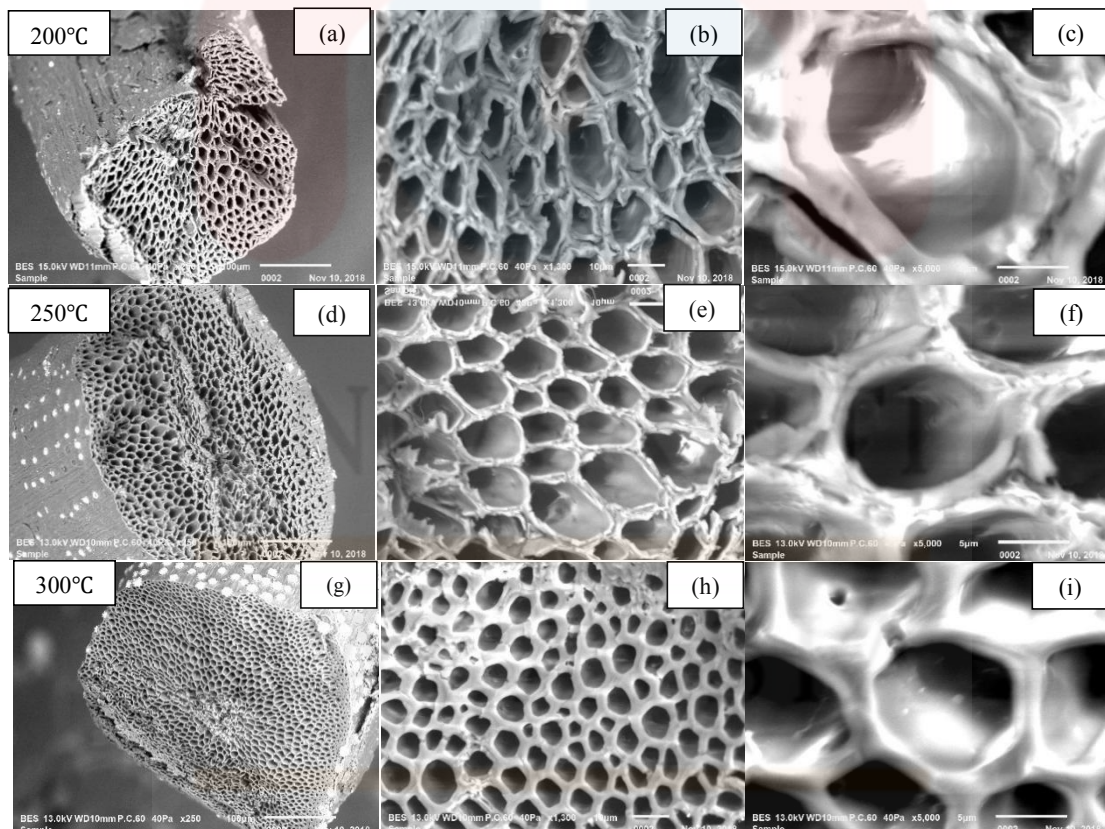


Figure 4.12: SEM images of torrefied OPEFB biochar surface structure on 60 minutes of torrefaction at respective holding temperatures with magnifications of x250 (a, d and g), x1500 (b, e and h) and x5000 (c, f and i)

SEM images shown in Figure 4.12 illustrated the surface structure of torrefied OPEFB biochar with different magnification of x250, x1500 and x5000 respectively for 60 minutes of residence time. From the SEM images observed, the physical changes of torrefied OPEFB biochar had smoother fibre surface and bigger porosity as the residence time increases due to pretreatment process. The torrefaction process of OPEFB biochar is therefore necessary to open its structure and increase its digestibility and subsequently the degree of conversion (Anli, 2013).

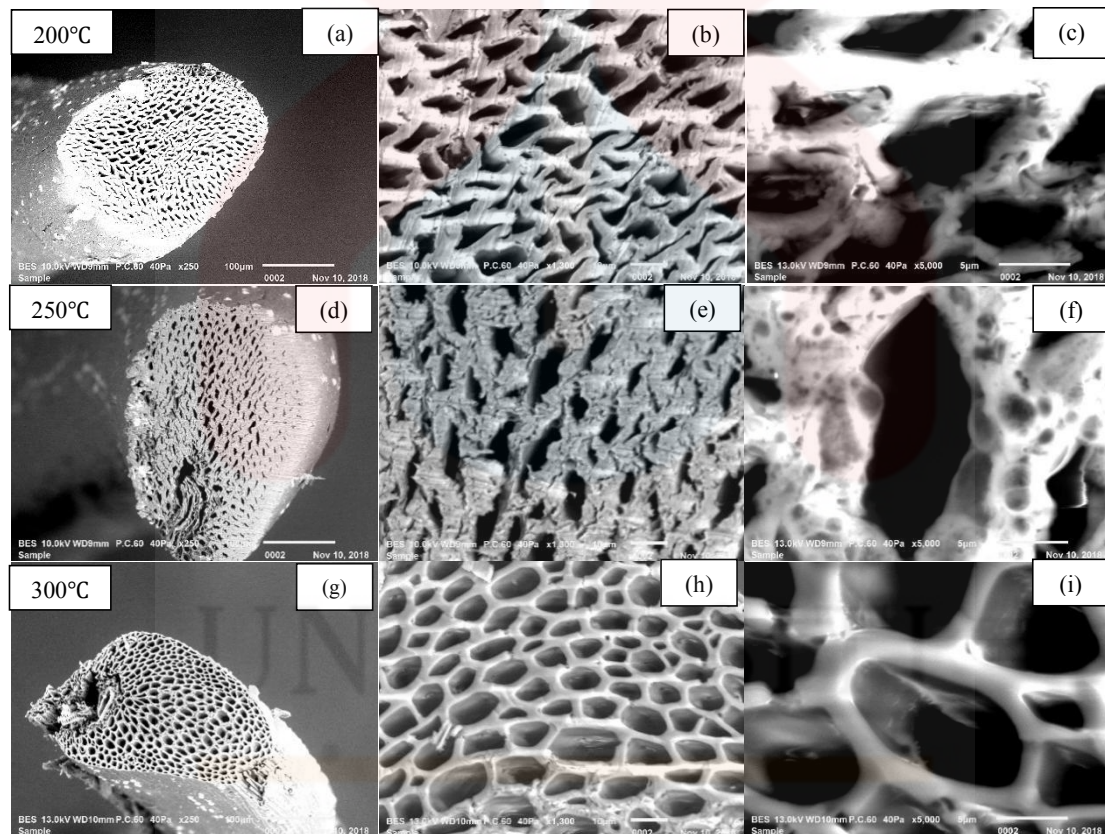


Figure 4.13: SEM images of torrefied OPEFB biochar surface structure on 90 minutes of torrefaction at respective holding temperature temperatures with magnifications of x250 (a, d and g), x1500 (b, e and h) and x5000 (c, f and i)

SEM images shown in Figure 4.13 illustrated the surface structure of torrefied OPEFB biochar with different magnification of x250, x1500 and x5000 respectively for 90 minutes. Physical changes can be seen clearly in both Figure 4.13(e) and

Figure 4.13(f) after being torrefied for 90 minutes, the morphological surface structure of the OPEFB biochar ruptured and the coarseness increase. This is due to the cell wall breakdown which can be clearly observed for biochar produced from the lowest ash content (0.3%) as stated in Table B.3. Thus, the porosity of the OPEFB biochar became decreases due to the thermochemical conversion.

4.7 Bonding Behaviour of Raw and Torrefied OPEFB Biochar

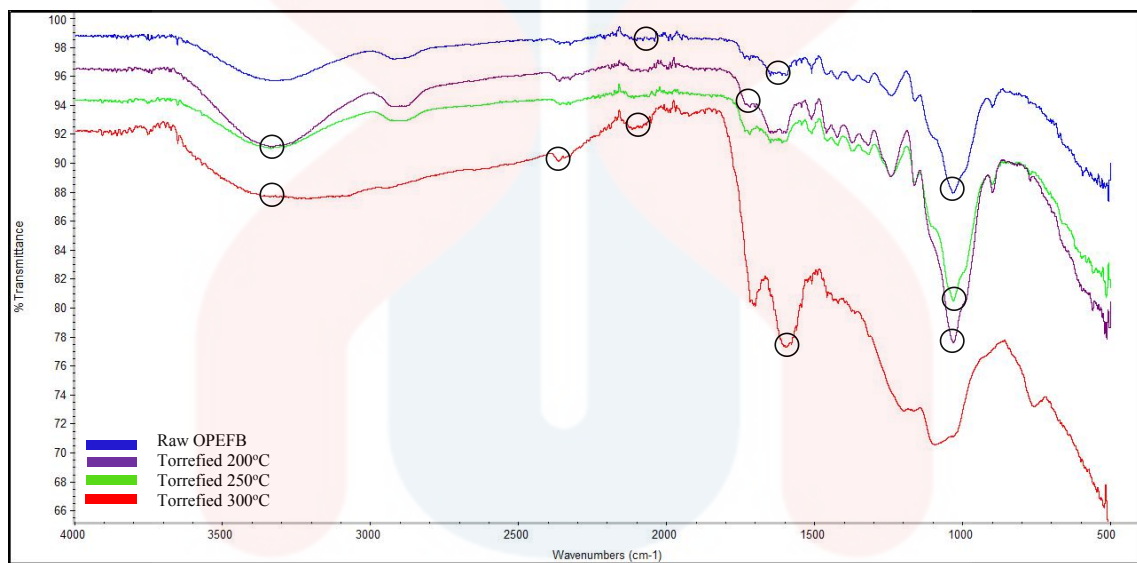
Fourier Transformation Infrared (FTIR) spectrometry have been used in this study to distinguish the change in chemical structure for both raw and torrefied OPEFB biochar by analyzed the functional groups, which later on will affected the degradation of hemicellulose, cellulose and lignin as of torrefaction impact. Generally, studying the functional group helped in determined the frequency of each lignocellulose to be degenerated (Iqbal et al., 2017).

The most common application of IR spectroscopy is to identify the functional groups and fingerprint region with the absorption bands $4000\text{--}1500\text{ cm}^{-1}$ and $1650\text{--}500\text{ cm}^{-1}$ region respectively. It is possible because different functional groups vibrate at different frequencies allowing their identification. However, the frequency of the vibration depends on additional factors such as delocalization of electrons, H-bonding and substitutions at the nearby groups.

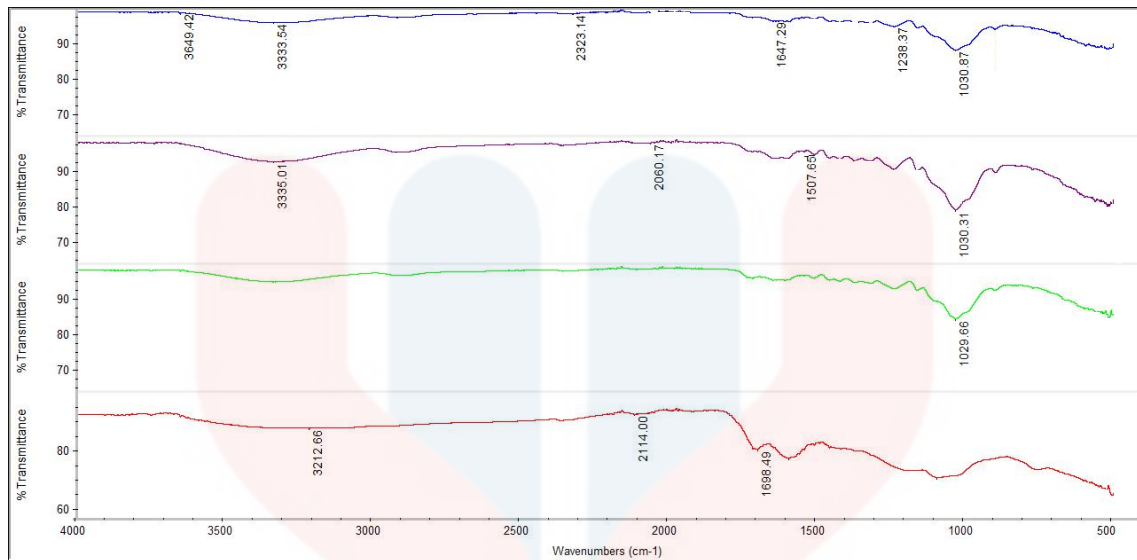
The lower energy portion of the mid-IR region ($1500 - 400\text{ cm}^{-1}$) usually contains a very complicated set of peaks arising due to complex vibrations involving several atoms. This region is unique to a particular compound and therefore is known as the fingerprint region of the IR spectrum. Though it is difficult to assign the

vibrational modes to these peaks, these are useful to identify a compound if the spectrum of the compound is already known.

In addition, the fingerprint region of the IR spectrum is unique to each compound. It is possible to identify a compound from its IR spectrum if the spectrum for the compound is already known and available for comparison. The wavenumbers for some of the bonds are shown in Figures 4.14 to Figure 4.16.



(a)

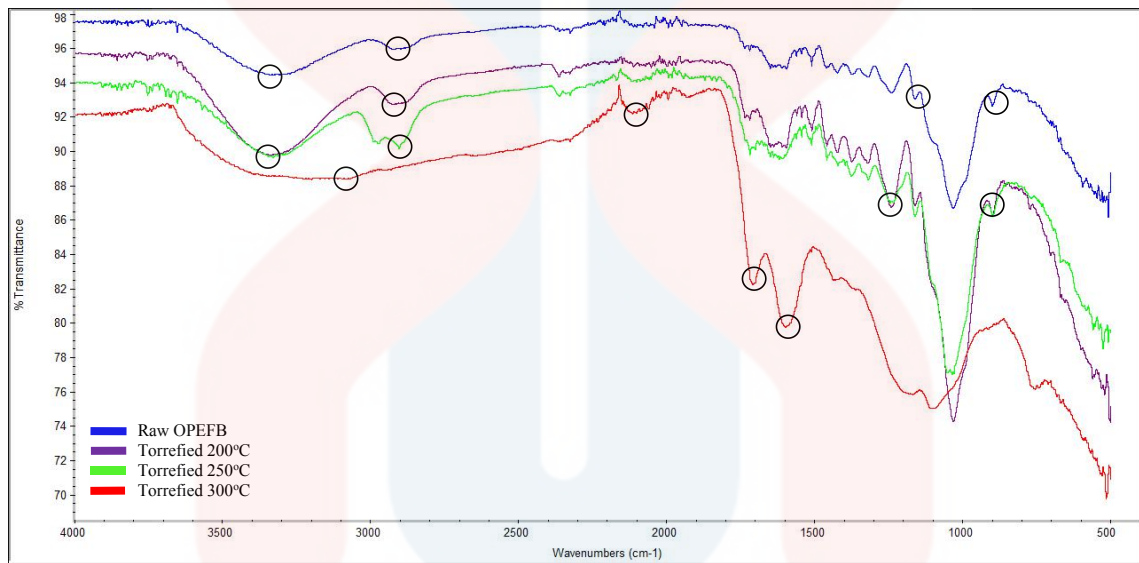


(b)

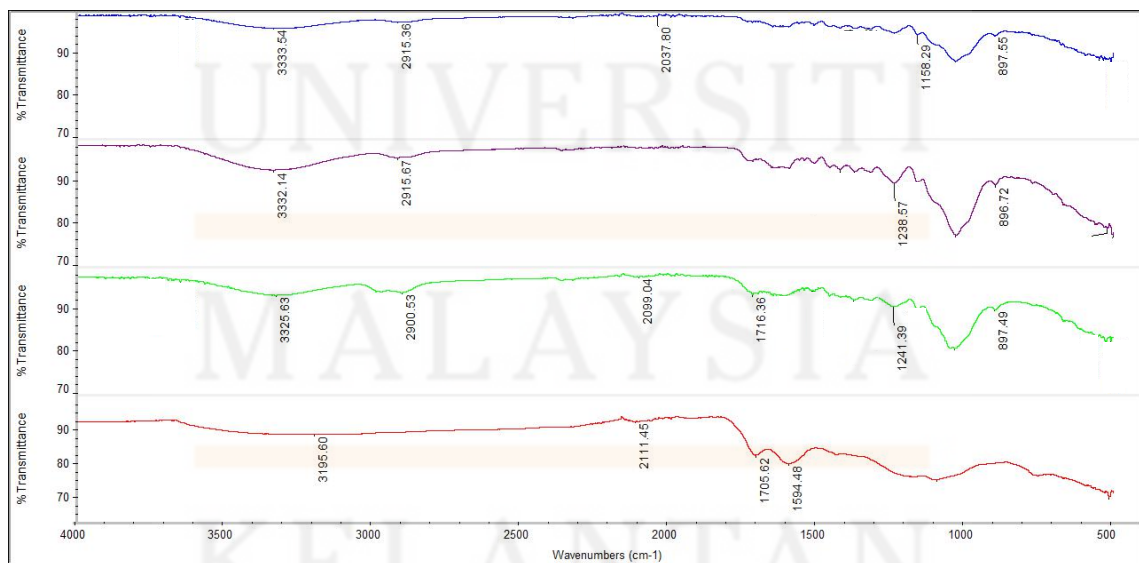
Figure 4.14: Functional groups presence during 30 minutes of torrefaction

Figure 4.14 show the IR spectrum displayed the functional groups identified during 30 minutes of torrefaction process on OPEFB biochar selected at different holding temperature of 200, 250 and 300°C respectively and being compared with the raw OPEFB fiber. From the result, it shows that peak at 2600-3450 cm^{-1} N-H bonds stretch at both raw and 200°C torrefied OPEFB biochar showing alkynes monosubstituted groups and started to diminish at higher torrefied temperature 250-300°C. There are inorganic phosphate, alkynes and aliphatic hydrocarbons presence where C=O and C-O identified from raw OPEFB fiber until 200°C torrefied OPEFB biochar then it was only alumino silicates where it also can be found C=O presence at 300°C torrefied OPEFB biochar at the strong band centered around peak 1698-3212 cm^{-1} which sometimes appears as one band and in other samples as multiple bands. There may also be bands due to associated water molecules around 3400 cm^{-1} and 1640 cm^{-1} . However a strong bond absorption was identified at 3212.66 cm^{-1} where O-H stretching presence. The valence vibration of

hydrogen-bonding of OH groups of cellulose I is the sum of three different hydrogen-bonds: intramolecular hydrogen bond of 2-OH...O-6, intramolecular hydrogen bond of 3-OH...O-5, intermolecular hydrogen bond of 6-OH...O-3 (Oh et al., 2005). Relative band-height at this region decreased as cellulose content decreased.



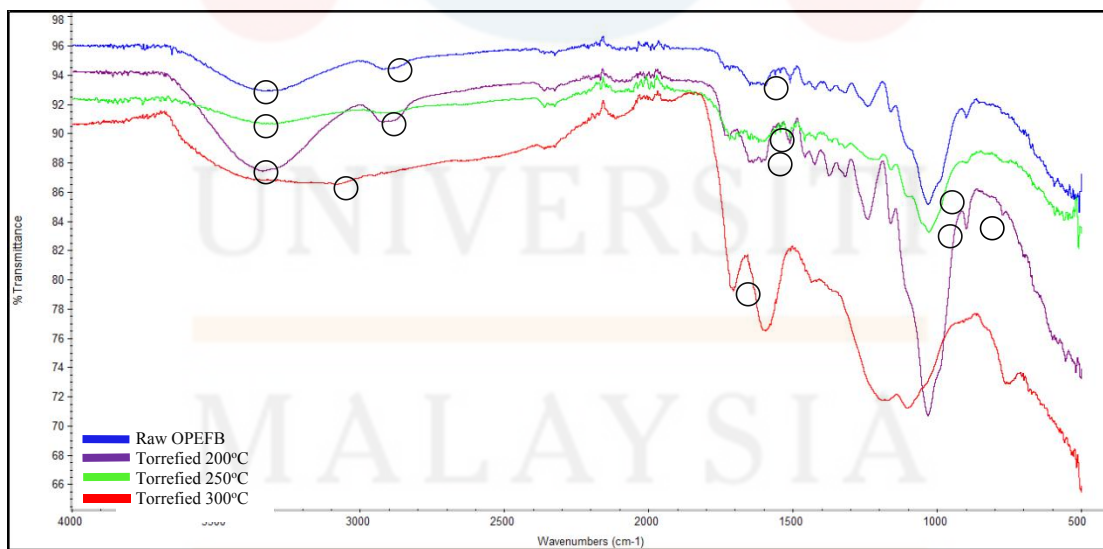
(a)



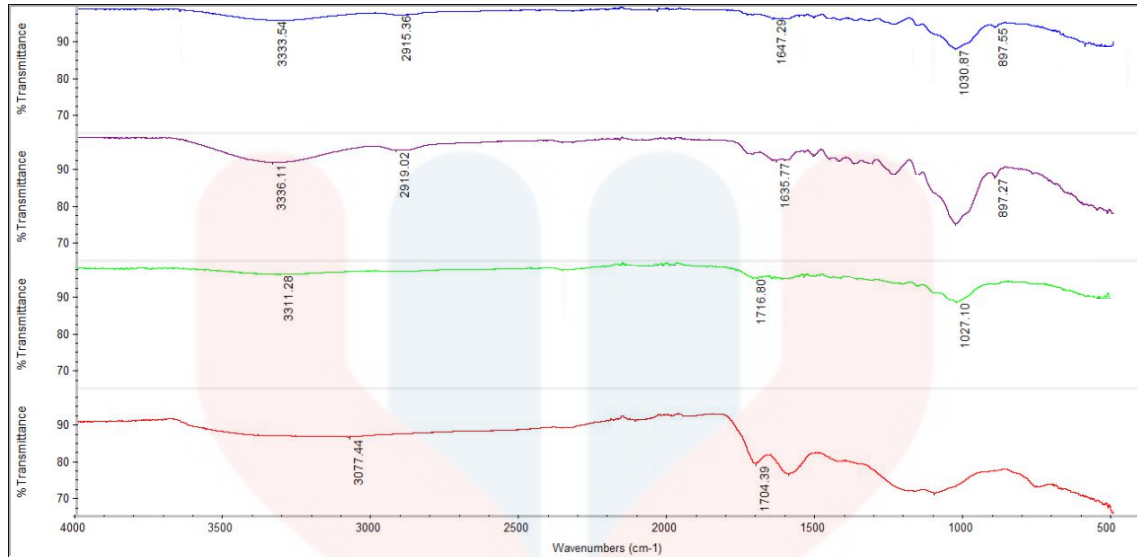
(b)

Figure 4.15: Functional groups presence during 60 minutes of torrefaction

Figure 4.15 show the IR spectrum displayed the functional groups identified during 60 minutes of torrefaction process on OPEFB biochar selected at different holding temperature of 200, 250 and 300°C respectively and being compared with the raw OPEFB fiber. The functional groups presence during 60 minutes of torrefaction time for the raw biomass, 200 and 250°C torrefied OPEFB biochar showing the same which is alkynes monosubstituted where C-H bond were identified at 3325.63-3333.64 cm^{-1} , aliphatic hydrocarbon group where N-H stretch (2900.53-2915.36 cm^{-1}) and C-O bond on inorganic phosphate (897.49-1241.39 cm^{-1}). However at 300°C torrefied OPEFB biochar only alumino silicate at peak 1534.48 cm^{-1} with C=O stretch and aliphatic carboxylic acid presence at peak 3195.60 cm^{-1} . Carboxylic acids normally exist in a dimeric form with very strong hydrogen bonds between the carbonyl and hydroxyl groups. This association results in the very broad, unusual -OH stretching absorption.



(a)



(b)

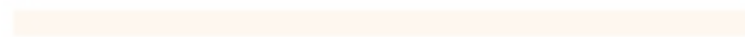
Figure 4.16: Functional groups presence during 90 minutes of torrefaction

Figure 4.16 show the IR spectrum displayed the functional groups identified during 90 minutes of torrefaction process on OPEFB biochar selected at different holding temperature of 200, 250 and 300°C respectively and being compared with the raw OPEFB fiber. Based on the result, during 90 minutes of torrefaction time the raw biomass and 200°C torrefied OPEFB biochar showing the same functional groups which is alkynes monosubstituted (897.27 and 3336.54 cm^{-1}), aliphatic hydrocarbon (2929.02 cm^{-1}) and inorganic phosphate (1030.87 cm^{-1}) where both N-H stretching, and C-N were presence, respectively. However there additional functional group identified which is the primary aliphatic alcohols at peak 1100-2900 cm^{-1} where strong C=O was identified. Alcohols contain the very polar -OH group where it allows hydrogen bonding between molecules in the condensed phase. Due to this hydrogen bonding, Jay & John (2002), stated that the boiling points of alcohols are much higher than the corresponding alkane with the same number of carbon atoms.

All the functional groups were absent as the holding temperature increased to 300°C where only aluminosilicates identified at peaks 1704.38 cm^{-1} and 3077.44 cm^{-1} where N-H stretching and C=O, respectively.



UNIVERSITI



MALAYSIA



KELANTAN

CHAPTER 5

CONCLUSION AND RECOMMENDATIONS

5.1 Conclusion

EFB is suitable for utilisation as a feedstock in the production of biochar via torrefaction. After taking into consideration on the independence variable and also its response on the properties of the torrefied OPEFB biochar produced, the particle size does not give any significant effect on the energy content properties of the biochar. From the response surface method, holding temperature at 300°C and 90 minutes of residence time give the most optimized on its calorific value.

Moreover, both surface morphology and bonding behaviour of the torrefied OPEFB was influenced by the degradation of the lignocellulose, hemicellulose, cellulose and lignin. Out of all torrefied OPEFB biochar produced in this study, at 300°C, 60min showed the high porosity while at 90 minutes of torrefaction process, the surface morphology of the biochar portrayed that it started to ruptured due to longer period of thermochemical reaction process as shown in Figure 4.10 to Figure 4.13.

5.2 Recommendations

There are several recommendations need to be considered and improved for the future study. Firstly other than EFB, there are abundance of biomass from oil palm mill waste such as OPT, OPF, OPKS which can be treated and produced biochar.

Future study can studies on these waste in order to compare the effectiveness of the biochar from EFB and other oil palm biomass.

Recent studies have been using furnace in order to produce the torrefied biochar which is heat was released during the process, but in future study, another treatment can be used to produce the biochar such by using a wave irradiation by microwave.

Lastly, during the torrefaction process, ceramic crucible have been used to place the OPEFB fiber to let it burn in the furnace and it might be one of the factor that affect the properties of the biochar produced. An alumina crucible can be replaced with the ceramic crucible since it is an extremely high mechanical strength and have a very high compressive strength due to its high hardness.

REFERENCES

- Abdullah, N., Bridgwater, A.V., (2006). Pyrolysis liquid derived from oil palm empty fruit bunches. *J. Phys. Sci.* 17, 117-129
- Abdullah, N., Gerhauser, H., Bridgwater, A. V., (2007), Bio-oil from Fast Pyrolysis of Oil Palm Empty Fruit Bunches, *Journal of Physical Science*, Vol.18, No.1, pp. 57-74, ISSN 1992-1950
- Abdullah, N., Gerhauser, H., (2008). Bio-oil derived from empty fruit bunches. *Fuel* 87 (12), 2606-2613
- Adialah, S., Syairah, M. & Nurhayati, A., (2014). Slow Pyrolysis of Oil Palm Empty Fruit Bunch for Biochar Fruit Bunches Production and Characterization. *Journal of Physical Science*. Vol. 25(2), 97-122. Retrieved from: https://www.researchgate.net/publication/301488610_Slow_Pyrolysis_of_Oil_Palm_Empty_Fruit_Bunches_for_Biochar_Production_and_Characterisation/download
- Adilah, S., Nurhayati, A. & Syairah, A., (2014). Slow Pyrolysis of Oil Palm Empty Fruit Bunches for Biochar Production and Characterisation. *Journal of Physical Science*. 25(2):97-112
- A.Khalil, M. S. Alwan., R. Ridzuan., H. Kamarudin & A. Khairul (2008). Chemical Composition, Morphological Characteristics, and Cell Wall Structure of Malaysian Oil Palm Fibers. *Polymer-Plastics Technology and Engineering*, 47:3, 273-280. Retrieved at: <http://dx.doi.org/10.1080/03602550701866840>
- Agensi Inovasi Malaysia (AIM), Kuala Lumpur (2015). New wealth creation for Malaysia's biomass industry: National Biomass Strategy 2020. Version 2.0, 2013. Available at: http://etp.pemandu.gov.my/upload/Biomass_Strategy_2013.pdf
- Akowuah, J. O., Kemausuor, F., & Mitchual, S. J., (2012). Physico-chemical characteristics and market potential of sawdust charcoal briquette. *International Journal of Energy and Environmental Engineering*
- Amin, N. A. S., Asmadi, M., (2008), Optimization of Empty Palm Fruit Bunch Pyrolysis over HZSM-5 Catalyst for Production of Bio-oil, In: *Universiti Teknologi Malaysia*, 5 March 2011, Available from: <http://eprints.utm.my/5125>
- Arias, B., Pedida, C., Ferosa, J., Plaza, M. G., Rubiera, F., Pis, J. J., (2008). Influence of torrefaction on the grindability and reactivity of woody biomass. *Fuel Process Technol* j 89(2):169-175
- H. Ariffin, M.A. Hassan, M.S. Umi Kalsom, N. Abdullah & Y. Shirai (2008). Effect of physical, chemical and thermal pretreatments on the enzymatic hydrolysis of oil palm empty fruit bunch (OPEFB). *J. Trop. Agric and Fd. Sc.* 36(2):000
- Bevan, N. B., Arshad A., Anwar J. , Amran T. A., & Oladokuna, O., (2018). Torrefaction of Pelletized Oil Palm Empty Fruit Bunches. *The 21st International Symposium on Alcohol Fuels – 21st ISAF*

- Basu, p., (2013). Biomass gasification, pyrolysis and torrefaction: practical design and theory. Academic Press..
- BioEnergy Consult (BEC), Malaysia, 2015. Bioenergy developments in Malaysia. Retrieved at: <http://www.bioenergyconsult.com/bioenergy-developments-malaysia>
- Bhattacharya, S. C., (2003). Biomass energy and densification: A global review with emphasis on developing countries. Energy Program, Asian Institute of Technology. p. 1–17.
- British Petroleum (BP), 2008. Statistical review of world energy. British: BP Plc
- Bregman, P. C. A., Boersma, A. R., Zwart, R. W. H., and Kiel, J. H. A., (2005). Torrefaction for biomass co-firing in existing coal-fired power stations. Report ECN-C-05-013, ECN
- Bridgeman, T. G., Jones, J. M., Sheild, I., Williams, P. T., (2008). Torrefaction of reed canary grass, wheat straw and willow to enhance solid fuel qualities and combustion properties. J Fuels 87:844-856
- Cheng, W. H., Lu, K. M., Lee, W. J., Liu, S. H., and Lin, T.C., (2014). Non-oxidative and oxidative torrefaction characterization and SEM observations of fibrous and ligneous biomass. Applied Energy, 114, 104–113
- Chew, J. J., Doshi, V., (2011). Recent advances in biomass pretreatment-torrefaction fundamentals and technology. Renew Sust Energ Rev:15(2011)4212-4222
- Chew, J.J., Doshi, V., Yong, S.T., and Bhattacharya, S. (2016). Kinetic study of torrefaction of oil palm shell, mesocarp and empty fruit bunch. Journal of Thermal Analysis and Calorimetry 126, 709-715
- Dodić, S. N., Popov, S. D., Dodić, J. M., Ranković, J. A., Zavargo, Z. Z., and Golusić, M. T., (2010). An overview of biomass energy utilization in vojvodina. Renewable and Sustain-able Energy Reviews; 14(1):550–3.
- Edward S. L., James R. A., and Thomas B. R., (2002). Enhanced Wood Fuels via Torrefaction. Fuel Chemistry Division Preprints 2002, 47(1), 408.
- Ellis, S., and Paszner, L., (1994). Activated self bonding of wood and agricultural residues. Holzforschung, 48; 82-90.
- Economic Planning Unit (EPU), Malaysia (2016). 11TH Malaysian Plan (2016-2020). Retrieved from: <http://www.rmk11.epu.gov.my/pdf/>
- Energy Commission (ST), Malaysia, 2015. Malaysia Energy Statistics Handbook. Retrived at: <http://www.st.gov.my>
- Energy Information Administration (EIA), (2013). Oil Marketing and Trading International (MTI), Malaysia oil market overview. Retrieved at: <http://www.oil-marketing.com/index.php/news/114-eia-malaysia-oil-market-overview>
- Energy Information Administration (EIA), 2015. International Energy Outlook. Retrieved at: <http://www.eia.gov>
- Fatih, D. M., Balat, M. & Balat H., (2009). Potential contribution of biomass

- G. Anli., (2013). Conversion of Oil Palm Empty Fruit Bunch to Biofuels, Liquid, Gaseous and Solid Biofuels, Zhen Fang, IntechOpen, DOI: 10.5772/53043. Available from:<https://www.intechopen.com/books/liquid-gaseous-and-solid-biofuels-conversion-techniques/conversion-of-oil-palm-empty-fruit-bunch-to-biofuels>
- Gan, P. Y., and Li, Z.,(2008). An econometric study on long-term energy outlook and the implications of renewable energy utilization in Malaysia. *Energy Policy*: 36:890–9.
- Goh, C. S., Tan, K. T., Lee, K. T., and Bhatia, S., (2010). Bio-ethanol from lignocellulose: status, perspectives and challenges in Malaysia. *Bioresource Technology*:4834–41.
- Hassan, M. A., Shirai, Y., (2003). Palm biomass utilization in Malaysia for the production of bioplastic. Retrieved at: http://www.biomass-asia-workshop.jp/presentation_files/21_AliHassan.pdf
- Hussain, A., Ani, F. N., Darus, A. N., Mokhtar, H., Azam, S., Mustafa, A., (2006), Thermochemical Behaviour of Empty Fruit Bunches and Oil Palm Shell Waste in Circulating Fluidized-Bed Combustor (CFBC), *Journal of Oil Palm Research*, Vol.18, No. 1, (June 2006), pp. 210-218, ISSN 1511-2780.
- Hussain, A. B., & Hamisham, H., (2016). Non-Renewable and Renewable Energy for Sustainable Electricity Generation in Malaysia. *World Academy of Science, Engineering and Technology. International Journal of Environmental and Ecological Engineering*. Vol. 10, No. 9 in lignocellulosic biomass pretreatment.
- International Energy Agency (2018). *Energy Efficiency: Industry. The Efficient World Scenario identifies opportunities in several industry sub-sectors*. Retrieved from:<https://www.iea.org/topics/energyefficiency/industry/>
- Ibrahim, R. H. H., Darvell, L. I., Jones, J. M., and Williams, A., (2013). Physicochemical characterisation of torrefied biomass. *Journal of Analytical and Applied Pyrolysis*, 103, 21–30.
- Jay, A. L. & John, E. B., (2002). Understanding and Exploiting C-H bond activation. *Nature* 417, 507-514
- Jaya, S. T., S. Sokhansanj., J. R., Hess, T. W., Wright, and R. D. Boardman., (2011). A review on biomass torrefaction process and product properties for energy applications. Retrieved at: <https://bioenergy.inl.gov/JournalArticles/A-review-on-biomass-torrefaction-process-and-product-properties-for-renewable-energy-applications.pdf>
- Koppejan, J. & Loo, S. V., (2012). *The handbook of biomass combustion and co-firing*. Abingdon-on-Thames: Routledge
- Kurnia, J. C., Jangam, S. V., Akhtar, S., Sasmito, A. P., & Mujumdar, A. S., (2016). Advances in Biofuel Production from Oil Palm and Palm Oil Processing Wastes. A Review. *Biofuel Res. J.* 3(28), 332–346
- Kushairi, A., Loh, S. K., Azman, I., Elina, H., Meilina, O. A., Zainal, B., Razmah, G., Shamala, S. & Ghulam, K. P., (2018). Oil palm economic performance in Malaysia and R&D progress in 2017. *Journal of Oil Palm Research* Vol. 30 (2). P

- 163-196. Retrieved:
<http://jopr.mpob.gov.my/wp-content/uploads/2018/06/jopr30june2018-kushairi.pdf>
- Knoef, H. A. M., (2005). Practical aspects of biomass gasification, In: Handbook of biomass gasification, BTG biomass technology group BV, pp. , Druckerij Giehoorn ten Brink, ISBN 978-908-100-6811, Natherlands.
- L. Tripathi, A. K. Mishra, Dubey, C. B. Tripathi & P. Baredar, (2016). Renewable Energy: An Overview on its contribution in current energy scenario of India. Renewable and Sustainable Energy Reviews, Vol. 60, PP. 226-233
- M. Ministry of Housing and Local Government (KPKT), 2005. National Physical Plan. Retrieved from:<http://www.npptownplan.gov.my>
- MPOB, (2018a). Overview of the Malaysian Oil Palm Industry 2017. Retrieved from:
<http://palmoilis.mpob.gov.my/index.php/overview-of-industry/593-overview-of-industry-2017>
- MPOB, (2018b). A Summary of the Performance of the Malaysian Oil Palm Industry 2017. Retrieved from:
<http://bepi.mpob.gov.my/index.php/en/statistics/production/186-production-2018/851-production-of-oil-palm-products-2018.html>
- Malaysia Energy Commission (ST), 2016.. Malaysia Energy Statistic Handbook; 2016.
- McKendry, P., (2012). Energy production from biomass (part1): overview microbubble-microbe synergy for biomass processing: Application
- Mulakhudair, A.R., Hanotu, J., & Zimmerman, W., (2016). Exploiting of biomass. Bioresour. Technol. 83, 37–46
- Nithitron, K. & Suthum, P., (2011). Thermal Upgrading of Biomass as a Fuel by Torrefaction. Department of Mechanical Engineering, King Mongkut's University of Technology North Bangkok. International Conference on Environmental Engineering and Applications IPCBEE, Vol.17
- Ok, Y. S., Uchimiya, S. M., Chang, S. X., & Bolan, N., (2016). Biochar: Production, Characterization, and Applications. Urbanization, Industrialization and the Environment Series.
- Onnoja, E., and heela Chandren1 · Fazira Ilyana Abdul Razak1 · Naji Arafat Mahat1 · Roswanira Abdul Wahab1(2018). Oil Palm (*Elaeis guineensis*) Biomass in Malaysia: The Present and Future Prospects. Waste and Biomass Valorization. Retrieved from:<https://www.doi.org/10.1007/s12649-018-0258-1>
- Onoja, E., Sheela, C., Fazira, I. A. R., & Roswanira, A. B., (2018). Oil Palm (*Elaeis guineensis*) Biomass in Malaysia: The Present and Future Prospects. Available from:https://www.researchgate.net/publication/323496339_Oil_Palm_Elaeis_guineensisBiomass_in_Malaysia_The_Present_and_Future_Prospects
- Oramahi, H. A. & Diba, F., (2013). Maximizing the Production of Liquid Smoke from Bark of Durio by Studying Its Potential Compounds. Procedia Environmental Sciences.13; 17: 60-69

- Paoluccio, A. J., Smith, R. S. & Modesto, C. A., (2006). U.S. patent application for method and apparatus for biomass torrefaction, manufacturing a storable fuel from biomass and producing offsets for the combustion products of fossil fuels and combustible article of manufacture. Docket no. 60/747,803.
- Pimchuai, A., Dutta, A. & Basu, P., (2010). Torrefaction of agricultural residue to enhance combustible properties. *Energy Fuel J* 24(9):4638-4645.
- Prins, M. J., (2005). Thermodynamic analysis of biomass gasification and torrefaction. Eindhoven: Technische University Eindhoven
- Rahman, A. A., Abdullah, N., & Sulaiman, F., (2014). Temperature effect on the characterization of pyrolysis products from oil palm fronds. *Adv. Energy Eng.* 2, 14
- Ridzuan, R., Stephen, S., and Mohd, A J., (2002). Properties of medium density fibreboard from oil palm empty fruit bunch fibre. *Journal Of Oil Palm Research*, 14(2); 34-40.
- Sadaka, S., & Negi, S., (2009). Improvements of biomass physical and thermochemical characteristics via torrefaction process. *Environmental Progress Sustainable Energy* 28(3), 427–434. doi: 10.1002/ep.10392.
- Samiran, N. A., Jaafar, M. N. M., Chong, C. T., & Jo-Han, N., (2015). A Review of Palm Oil Biomass as a Feedstock for Syngas Fuel Technology. *J. Teknologi. Sci. Eng.* 72, 13–18 (2015) sustainable energy development. *Energy Conversion and Management*;50(7):1746–60.
- M. Shafie., T. M. I. Mahli., H. H. Masjuki., & A. A. Yazid., (2011). A review on electricity generation based on biomass residue in Malaysia: Renewable and Sustainable Energy Reviews 16 (2012) 5879–5889. Retrieved at: https://umexpert.um.edu.my/file/publication/00003184_85080.pdf.
- Sun Y., Liu J., Kennedy J. F. Application of Response Surface Methodology for Optimization of Polysaccharides Production Parameter from the Roots of *Codonopsis pilosula* by a Central Composite Design. *J Carbohydrate Polymers* 2010; 80: 949–953.
- The Malaysia Economic in Figures, (2010). Economic planning unit. Prime Minister Department. Retrieved from: <http://www.epu.gov.my/malaysianeconomyfigures2009>.
- Tenaga Nasional Berhad (TNB), 2016. Annual Report 2016
- Tick, H. O., Shen, Y. P. & Shing, C. C., (2010). Energy policy and alternative energy in Malaysia: Issues and challenges for sustainable growth. *Renewable and Sustainable Energy Reviews* 14.1241–1252. Retrieved at: <https://www.sciencedirect.com/science/article/pii/S1364032109002834>
- Wahid, M. B., Abdullah, S. N. A., & Henson, I. E., (2009). Oil palm e achievements and potential. *New Directions for a diverse planet*. In: Proceedings of the fourth international crop science congress, Brisbane, Australia; 26 Sepel Oct 2004. Retrieved from: <http://www.cropscience.org.au>

Zanzi, R., Ferro, D. T., Torres, A., Soler, P. B., & Bjornbom, E., (2002). Biomass Torrefaction. The 6th Asia-Pacific International Symposium on Combustion and Energy Utilization. Kuala Lumpur, Malaysia.



UNIVERSITI



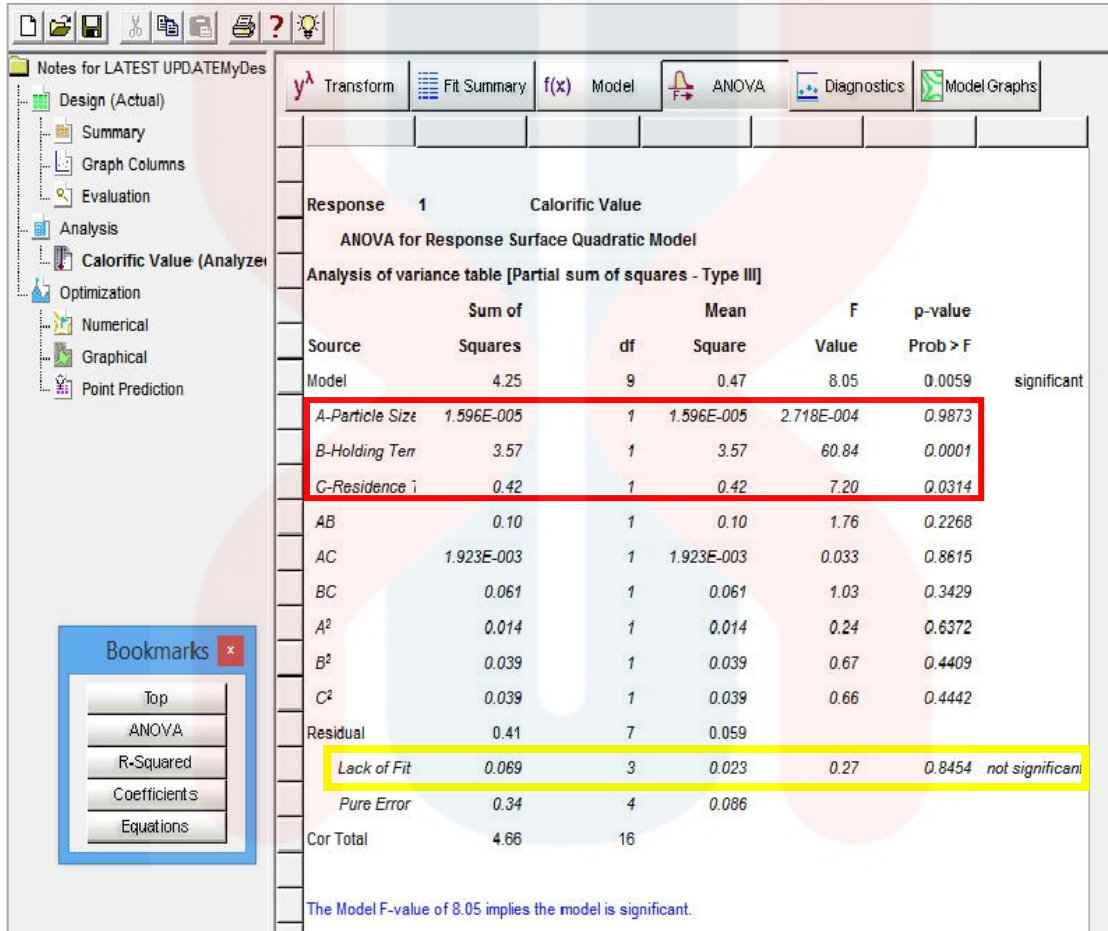
MALAYSIA



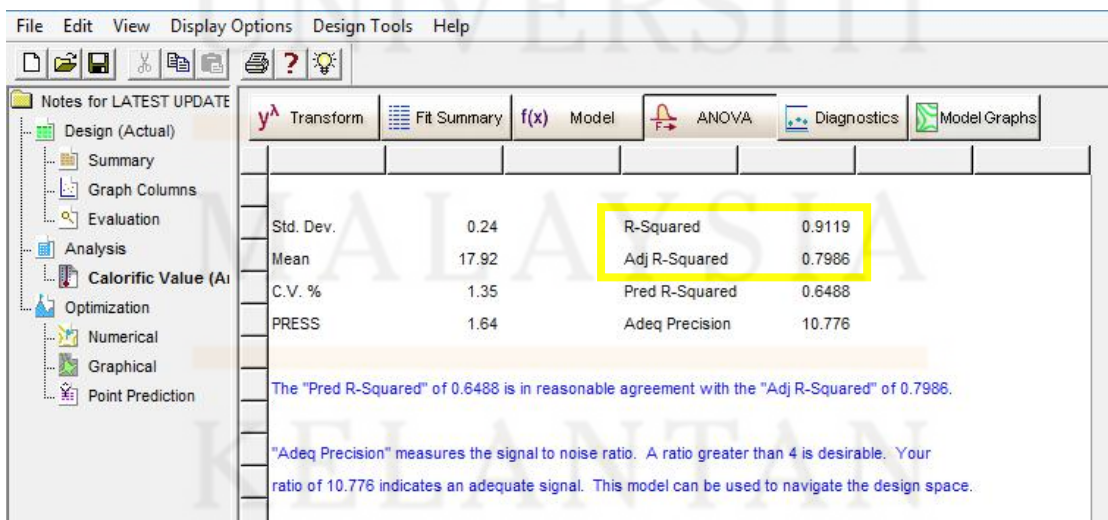
KELANTAN

APPENDIX

APPENDIX-A



(a)



(b)

Figure A.1: (a) ANOVA for response surface of calorific value and (b) R² and Adj R² value

APPENDIX-B

Table B.1: Heating rate of torrefaction

Run	Factor 1 Particle Size (µm)	Factor 2 Holding Temp. (°C)	Factor 3 Residence Time (min)	Furnace Starting Temp. (°C)	Temp. Before Starting Residence Time (°C)	Residence Time (min)	Heating Rate (°C/min)	Time to Reach Temp. Before Starting Residence Time (min)
1	250	250	90	49	253	90	6.58	31
2	500	300	30	41	305	30	9.10	29
3	750	250	90	45	251	90	7.92	26
4	500	250	60	36	254	60	8.38	26
5	750	250	30	49	249	30	8.33	24
6	500	250	60	43	251	60	8.67	24
7	250	250	30	40	252	30	10.10	21
8	500	200	90	42	201	90	7.95	20
9	500	250	60	44	251	60	9.86	21
10	750	300	60	50	303	60	7.91	32
11	250	200	60	35	202	60	5.96	28
12	750	200	60	47	201	60	6.42	24
13	500	250	60	46	253	60	9.41	22
14	250	300	60	75	299	60	8.76	29
15	500	250	60	45	252	60	8.28	25
16	500	300	90	49	278	90	9.96	23
17	500	200	30	48	204	30	9.75	16

Table B.2: Mass yield

Run	Factor 1 Particle Size (µm)	Factor 2 Holding Temp. (°C)	Factor 3 Residence Time (min)	Initial Weight (g)	Final Weight (g)	Mass Yield (%)
1	250	250	90	5.0005	3.4351	68.6951
2	500	300	30	5.0014	2.1684	43.3559
3	750	250	90	5.0003	3.4785	69.5658
4	500	250	60	5.0005	3.7904	75.8004
5	750	250	30	5.0003	4.1390	82.7550
6	500	250	60	5.0001	3.8337	76.6725
7	250	250	30	5.0007	4.3566	87.1198
8	500	200	90	5.0001	4.5926	91.8502
9	500	250	60	5.0001	3.9780	79.5584
10	750	300	60	5.0017	1.7396	34.7802
11	250	200	60	5.0004	4.6977	93.9465
12	750	200	60	5.0006	4.8933	97.8543
13	500	250	60	5.0009	3.4173	68.3337
14	250	300	60	5.0025	1.5735	31.4543
15	500	250	60	5.0002	4.0121	80.2388
16	500	300	90	5.0008	1.5876	31.7469
17	500	200	30	5.0008	4.6870	93.77250

Table B.3: Proximate Analysis Data

SAMPLE	UNIT	TEST				
		MOISTURE CONTENT	VOLATILE CONTENT	ASH CONTENT	FIXED CARBON	CV
1	%	13.88	81.54	0.30	4.28	16.9508
2	%	9.10	74.41	1.65	14.84	18.3672
3	%	10.84	51.53	3.02	34.61	19.1211
4	%	7.83	73.70	1.68	16.79	18.0437
5	%	7.64	79.81	1.36	11.19	17.7141
6	%	7.73	79.89	1.14	11.24	17.5772
7	%	7.82	81.80	2.02	8.36	17.7884
8	%	9.65	82.40	1.52	6.43	17.2736
9	%	10.86	47.77	4.75	36.62	18.7780
10	%	9.23	83.24	1.48	6.05	17.2328
11	%	9.29	81.75	1.44	7.52	17.1847
12	%	11.05	47.34	5.25	36.36	18.2939
13	%	11.43	69.62	3.98	14.97	18.3775
14	%	10.76	82.91	2.52	3.81	17.2230

Table B.4: Effect of holding temperature and residence time on moisture content

Holding Temperature (°C)	Residence Time (min)		
	30	60	90
200	11.43	10.86	9.98
250	10.76	9.65	9.23
300	9.1	8.46	7.83

Table B.5: Effect of holding temperature and residence time on volatile content

Holding Temperature (°C)	Residence Time (min)		
	30	60	90
200	83.24	81.91	80.4
250	79.81	76.89	73.7
300	60.62	51.53	47.77

Table B.6: Effect of holding temperature and residence time on ash content

Holding Temperature (°C)	Residence Time (min)		
	30	60	90
200	1.14	1.36	1.65
250	1.48	1.82	2.52
300	3.02	3.98	4.75

Table B.7: Effect of holding temperature and residence time on fixed carbon

Holding Temperature (°C)	Residence Time (min)		
	30	60	90
200	4.19	5.87	8.03
250	7.95	11.64	14.55
300	27.76	36.03	39.65

Table B.8: Effect of holding temperature and residence time on calorific value

Holding Temperature (°C)	Residence Time (min)		
	30	60	90
200	17.223	17.3328	17.4736
250	17.5772	17.7141	18.1672
300	18.3775	18.778	19.1211

Table B.9: Burning phase experiment 1

Time	Temp.	Time	Temp.	Time	Temp.	Phase (min)
0	50	45	251	90	253	
1	72	46	248	91	253	
2	90	47	249	92	250	
3	110	48	252	93	249	
4	128	49	253	94	250	
5	133	50	251	95	252	
6	131	51	249	96	252	
7	141	52	249	97	250	
8	160	53	251	98	249	
9	167	54	252	99	249	
10	174	55	252	100	251	
11	198	56	250	101	252	
12	196	57	248	102	251	
13	202	58	250	103	249	
14	218	59	252	104	249	
15	230	60	250	105	250	
16	249	61	249	106	252	
17	253	62	249	107	251	
18	251	63	250	108	250	
19	250	64	252	109	248	
20	251	65	251	110	249	
21	247	66	249	111	251	
22	247	67	251	112	252	
23	252	68	253	113	251	
24	251	69	251	114	249	
25	252	70	249	115	249	
26	248	71	249	116	250	
27	248	72	250	117	251	
28	252	73	252	118	251	
29	254	74	252	119	249	
30	253	75	250	120	248	
31	250	76	249	121	249	
32	248	77	249	122	252	
33	251	78	251	123	252	
34	253	79	252	124	249	
35	250	80	251	125	246	
36	248	81	249	126	243	
37	250	82	249	127	239	
38	253	83	250	128	236	
39	253	84	252	129	232	
40	250	85	252	130	229	
41	248	86	250	131	226	
42	249	87	248	132	223	
43	252	88	249	133	220	
44	253	89	252	134	217	

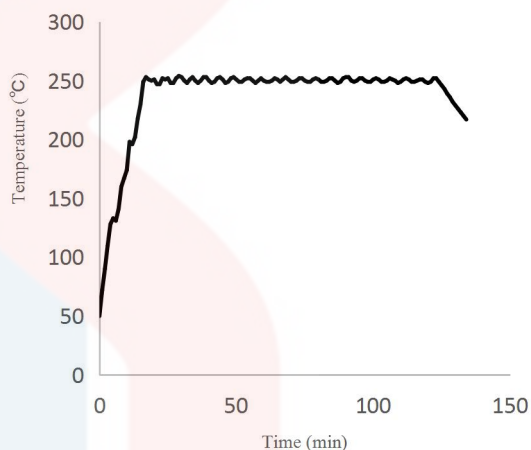


Table B.10: Burning phase experiment 2

Time	Temp.	Time	Temp.	Time	Temp.	Phase (min)
0	41	45	300	90	207	
1	52	46	299	91	205	
2	95	47	300	92	203	
3	101	48	303	93	202	
4	118	49	302	94	200	
5	124	50	299	95	197	
6	136	51	298	96	195	
7	136	52	300	97	193	
8	141	53	302	98	192	
9	162	54	302	99	190	
10	171	55	298			
11	188	56	300			
12	200	57	302			
13	213	58	301			
14	224	59	298			
15	227	60	298			
16	234	61	302			
17	246	62	301			
18	250	63	298			
19	268	64	292			
20	279	65	287			
21	279	66	281			
22	278	67	276			
23	293	68	270			
24	298	69	265			
25	299	70	260			
26	300	71	256			
27	298	72	252			
28	305	73	248			
29	300	74	245			
30	301	75	242			
31	305	76	239			
32	304	77	236			
33	299	78	234			
34	298	79	231			
35	301	80	228			
36	304	81	224			
37	301	82	223			
38	298	83	221			
39	298	84	218			
40	302	85	216			
41	304	86	214			
42	301	87	212			
43	298	88	210			
44	299	89	208			

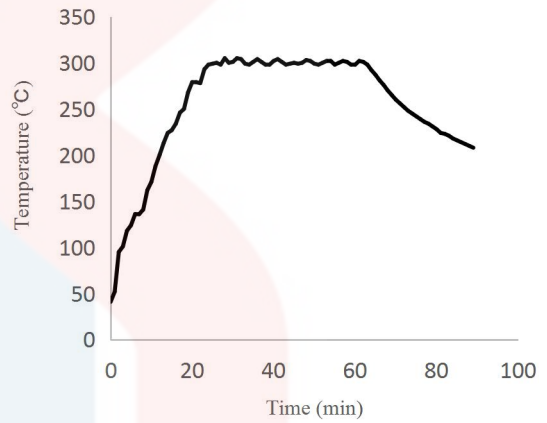


Table B.11: Burning phase experiment 3

Time	Temp.	Time	Temp.	Time	Temp.	Phase (min)
0	45	45	248	90	251	
1	45	46	250	91	251	
2	47	47	252	92	249	
3	60	48	253	93	248	
4	85	49	250	94	250	
5	107	50	249	95	252	
6	115	51	249	96	252	
7	123	52	252	97	250	
8	125	53	252	98	250	
9	125	54	251	99	250	
10	136	55	248	100	251	
11	154	56	248	101	249	
12	160	57	251	102	249	
13	181	58	254	103	250	
14	190	59	254	104	251	
15	193	60	251	105	251	
16	196	61	249	106	249	
17	215	62	250	107	248	
18	237	63	252	108	251	
19	246	64	252	109	250	
20	247	65	251	110	251	
21	255	66	248	111	250	
22	252	67	249	112	250	
23	253	68	251	113	249	
24	255	69	252	114	250	
25	251	70	251	115	251	
26	250	71	249	116	252	
27	253	72	250	117	251	
28	253	73	251	118	248	
29	250	74	251	119	247	
30	248	75	250	120	245	
31	248	76	250	121	242	
32	252	77	249	122	239	
33	254	78	249	123	236	
34	248	79	251	124	233	
35	248	80	252	125	230	
36	251	81	250	126	227	
37	253	82	249	127	224	
38	252	83	249	128	221	
39	249	84	250	129	218	
40	248	85	252	130	214	
41	250	86	252	131	213	
42	253	87	249	132	211	
43	253	88	249	133	209	
44	250	89	251	134	208	

Table B.12: Burning phase experiment 4

Time	Temp.	Time	Temp.	Time	Temp.	Phase (min)
0	36	45	253	90	244	
1	44	46	252	91	241	
2	56	47	250	92	237	
3	77	48	248	93	231	
4	90	49	250	94	228	
5	106	50	253	95	225	
6	117	51	252	96	221	
7	120	52	249	97	219	
8	126	53	248	98	216	
9	150	54	250	99	214	
10	156	55	253	100	211	
11	164	56	252	101	209	
12	171	57	249	102	207	
13	184	58	250	103	204	
14	199	59	252	104	203	
15	210	60	251	105	201	
16	229	61	249	106	199	
17	240	62	250	107	197	
18	242	63	251	108	194	
19	240	64	250	109	193	
20	251	65	251	110	192	
21	253	66	250	111	190	
22	252	67	252	112	189	
23	250	68	249	113	187	
24	249	69	248	114	186	
25	254	70	250	115	184	
26	250	71	253	116	183	
27	252	72	251	117	181	
28	254	73	249	118	180	
29	253	74	249			
30	249	75	253			
31	247	76	252			
32	251	77	250			
33	253	78	249			
34	250	79	250			
35	248	80	252			
36	253	81	252			
37	253	82	250			
38	251	83	248			
39	245	84	250			
40	244	85	251			
41	252	86	253			
42	253	87	251			
43	249	88	249			
44	251	89	248			

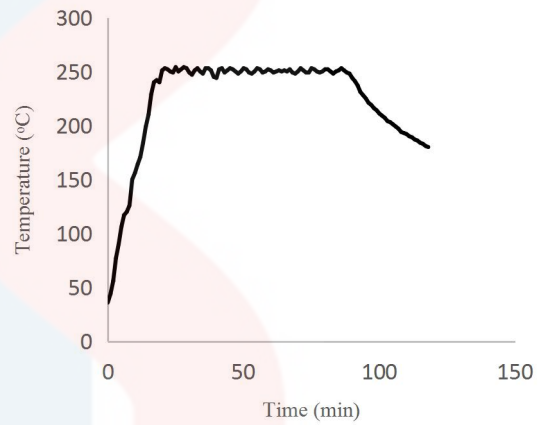


Table B.13: Burning phase experiment 5

Time	Temp.	Time	Temp.	Time	Temp.	Phase (min)
0	49	45	252			
1	50	46	254			
2	52	47	253			
3	56	48	249			
4	69	49	249			
5	92	50	250			
6	112	51	253			
7	125	52	252			
8	131	53	250			
9	134	54	248			
10	138	55	255			
11	155	56	253			
12	179	57	248			
13	193	58	244			
14	198	59	239			
15	199	60	235			
16	200	61	230			
17	213	62	227			
18	237	63	223			
19	252	64	220			
20	256	65	217			
21	254	66	211			
22	251	67	209			
23	249	68	206			
24	250	69	203			
25	252	70	199			
26	253	71	196			
27	249	72	194			
28	248	73	191			
29	249	74	189			
30	253	75	186			
31	252	76	185			
32	249	77	180			
33	248	78	180			
34	251	79	179			
35	253	80	178			
36	252	81	177			
37	250	82	175			
38	248	83	174			
39	250					
40	253					
41	253					
42	251					
43	248					
44	249					

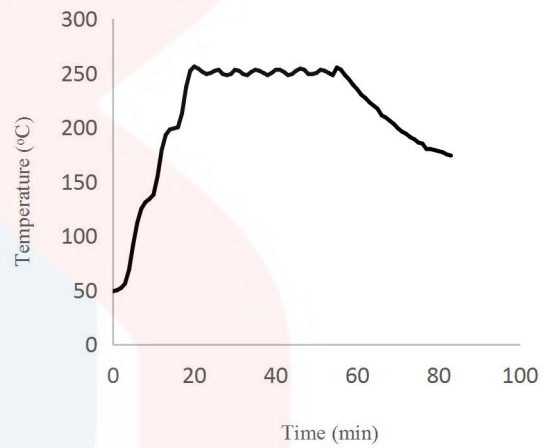


Table B.14: Burning phase experiment 6

Time	Temp.	Time	Temp.	Time	Temp.	Phase (min)
0	43	45	248	90	240	
1	46	46	251	91	232	
2	63	47	254	92	228	
3	96	48	253	93	225	
4	121	49	250	94	222	
5	116	50	248	95	219	
6	142	51	250	96	215	
7	144	52	252	97	212	
8	144	53	253	98	209	
9	142	54	251	99	207	
10	152	55	249	100	205	
11	178	56	249	101	203	
12	198	57	251	102	200	
13	207	58	253	103	198	
14	208	59	252	104	197	
15	206	60	249	105	194	
16	211	61	248	106	193	
17	214	62	250	107	192	
18	238	63	252	108	190	
19	258	64	252	109	188	
20	254	65	251	110	186	
21	252	66	249	111	185	
22	255	67	248	112	184	
23	251	68	250	113	182	
24	250	69	252	114	181	
25	252	70	252			
26	253	71	251			
27	251	72	249			
28	248	73	248			
29	247	74	253			
30	250	75	252			
31	254	76	250			
32	253	77	248			
33	250	78	252			
34	248	79	253			
35	250	80	251			
36	253	81	249			
37	253	82	250			
38	250	83	251			
39	248	84	248			
40	249	85	244			
41	253	86	240			
42	253	87	252			
43	251	88	248			
44	249	89	244			

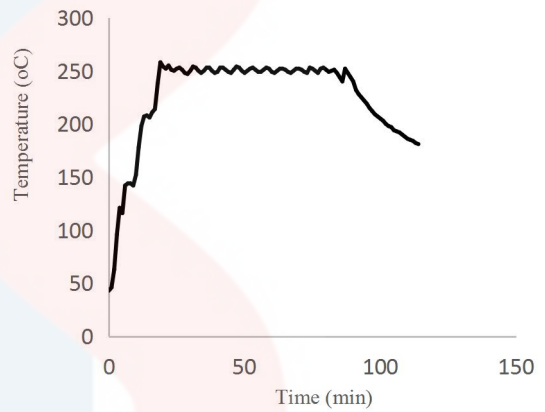


Table B.15: Burning phase experiment 7

Time	Temp.	Time	Temp.	Time	Temp.	Phase (min)
0	40	45	249			
1	42	46	250			
2	51	47	253			
3	81	48	249			
4	106	49	248			
5	124	50	250			
6	130	51	250			
7	138	52	251			
8	141	53	250			
9	149	54	246			
10	156	55	243			
11	167	56	238			
12	177	57	234			
13	198	58	230			
14	201	59	226			
15	216	60	223			
16	238	61	219			
17	251	62	216			
18	249	63	213			
19	252	64	210			
20	252	65	208			
21	251	66	205			
22	252	67	203			
23	253	68	200			
24	251	69	198			
25	247	70	196			
26	249	71	194			
27	252	72	192			
28	254	73	189			
29	251	74	187			
30	248	75	186			
31	251	76	184			
32	254	77	183			
33	252	78	181			
34	248	79	180			
35	251	80	179			
36	253					
37	253					
38	249					
39	248					
40	250					
41	253					
42	253					
43	250					
44	248					

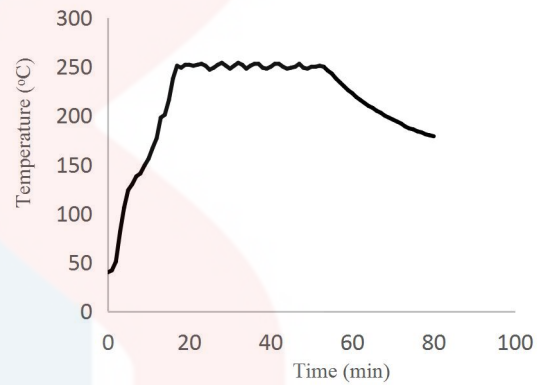


Table B.16: Burning phase experiment 8

Time	Temp.	Time	Temp.	Time	Temp.	Phase (min)
0	42	45	203	90	200	
1	42	46	201	91	202	
2	53	47	199	92	202	
3	87	48	199	93	200	
4	118	49	201	94	200	
5	135	50	203	95	200	
6	143	51	202	96	200	
7	146	52	200	97	200	
8	146	53	199	98	200	
9	144	54	200	99	199	
10	142	55	202	100	200	
11	146	56	203	101	201	
12	167	57	201	102	201	
13	171	58	199	103	200	
14	182	59	199	104	199	
15	199	60	200	105	198	
16	201	61	202	106	201	
17	203	62	202	107	203	
18	202	63	200	108	201	
19	201	64	201	109	202	
20	200	65	199	110	200	
21	201	66	199	111	199	
22	202	67	202	112	198	
23	202	68	203	113	197	
24	200	69	204	114	195	
25	198	70	202	115	193	
26	198	71	200	116	190	
27	202	72	199	117	188	
28	204	73	199	118	185	
29	203	74	201	119	183	
30	200	75	202	120	180	
31	202	76	202	121	178	
32	202	77	200	122	176	
33	201	78	199	123	174	
34	199	79	200	124	172	
35	198	80	201	125	170	
36	200	81	201	126	166	
37	201	82	200	127	164	
38	202	83	199	128	163	
39	203	84	199	129	161	
40	202	85	201	130	160	
41	199	86	202	131	158	
42	199	87	201	132	157	
43	200	88	200	133	155	
44	202	89	199	134	152	

Table B.17: Burning phase experiment 9

Time	Temp.	Time	Temp.	Time	Temp.	Phase (min)
0	44	45	252	90	226	
1	54	46	248	91	223	
2	79	47	250	92	220	
3	102	48	253	93	217	
4	115	49	252	94	213	
5	125	50	250	95	210	
6	128	51	253	96	208	
7	129	52	252	97	207	
8	130	53	250	98	204	
9	142	54	249	99	202	
10	167	55	250	100	200	
11	187	56	251	101	198	
12	196	57	250	102	196	
13	198	58	249	103	195	
14	197	59	250	104	193	
15	203	60	251	105	192	
16	225	61	251	106	190	
17	247	62	250	107	188	
18	255	63	249	108	187	
19	251	64	249	109	186	
20	250	65	250	110	184	
21	252	66	253	111	183	
22	249	67	251			
23	248	68	249			
24	249	69	249			
25	248	70	250			
26	249	71	253			
27	252	72	253			
28	254	73	251			
29	251	74	249			
30	249	75	249			
31	252	76	251			
32	251	77	252			
33	252	78	251			
34	252	79	249			
35	250	80	249			
36	248	81	249			
37	249	82	252			
38	253	83	250			
39	253	84	246			
40	251	85	244			
41	248	86	240			
42	248	87	237			
43	251	88	233			
44	253	89	229			

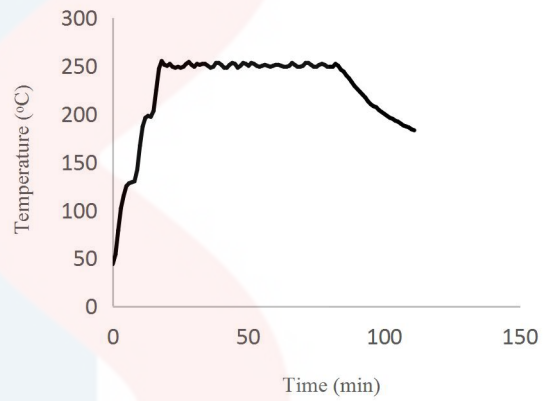


Table B.18: Burning phase experiment 10

Time	Temp.	Time	Temp.	Time	Temp.	Phase (min)
0	50	45	297	90	281	
1	52	46	300	91	277	
2	63	47	303	92	273	
3	88	48	302	93	269	
4	111	49	299	94	265	
5	138	50	298	95	261	
6	139	51	300	96	255	
7	139	52	303	97	249	
8	143	53	301	98	244	
9	160	54	298	99	242	
10	186	55	298	100	239	
11	198	56	301	101	237	
12	204	57	303	102	235	
13	204	58	301	103	232	
14	205	59	298	104	230	
15	217	60	299	105	228	
16	240	61	302	106	224	
17	256	62	302	107	222	
18	260	63	300	108	219	
19	259	64	298	109	217	
20	265	65	302	110	215	
21	288	66	302	111	213	
22	307	67	300	112	209	
23	302	68	298	113	208	
24	302	69	300	114	207	
25	301	70	302			
26	298	71	302			
27	302	72	299			
28	303	73	298			
29	298	74	300			
30	298	75	300			
31	302	76	301			
32	303	77	299			
33	297	78	298			
34	300	79	301			
35	297	80	302			
36	300	81	300			
37	302	82	299			
38	303	83	299			
39	300	84	301			
40	303	85	301			
41	301	86	299			
42	302	87	295			
43	303	88	291			
44	299	89	286			

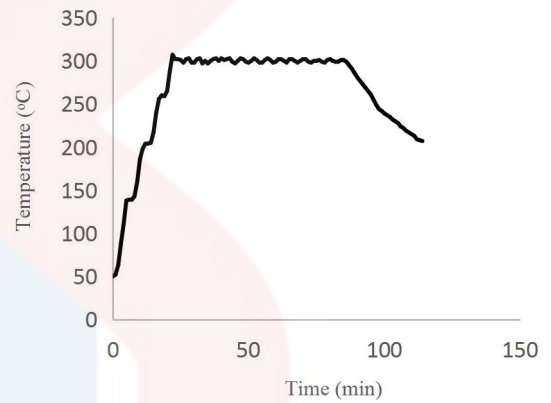


Table B.19: Burning phase experiment 11

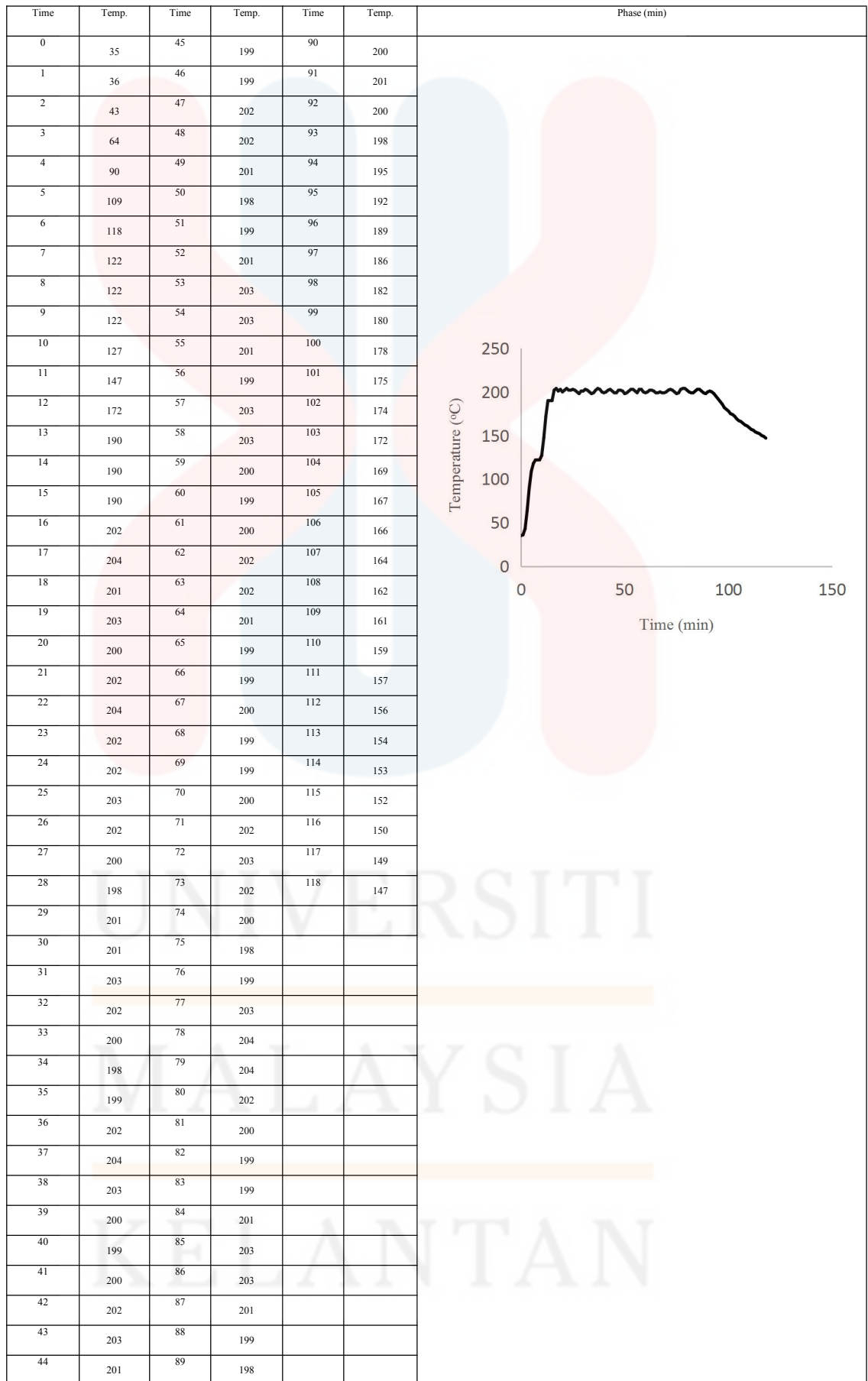


Table B.20: Burning phase experiment 12

Time	Temp.	Time	Temp.	Time	Temp.	Phase (min)
0	47	45	201	90	197	
1	51	46	201	91	194	
2	56	47	199	92	191	
3	61	48	199	93	189	
4	58	49	201	94	186	
5	69	50	202	95	184	
6	94	51	202	96	181	
7	113	52	201	97	179	
8	125	53	199	98	176	
9	129	54	201	99	174	
10	131	55	203	100	172	
11	132	56	202	101	170	
12	137	57	202	102	168	
13	156	58	201	103	166	
14	180	59	200	104	164	
15	194	60	199	105	163	
16	198	61	201	106	161	
17	198	62	203	107	159	
18	199	63	202	108	158	
19	205	64	201	109	156	
20	203	65	199	110	154	
21	201	66	199	111	152	
22	202	67	201	112	151	
23	205	68	203	113	150	
24	201	69	202			
25	200	70	201			
26	201	71	200			
27	203	72	199			
28	203	73	199			
29	200	74	201			
30	199	75	200			
31	199	76	199			
32	201	77	199			
33	203	78	201			
34	203	79	202			
35	200	80	202			
36	199	81	201			
37	199	82	199			
38	201	83	199			
39	202	84	201			
40	200	85	202			
41	199	86	204			
42	199	87	204			
43	201	88	203			
44	202	89	200			

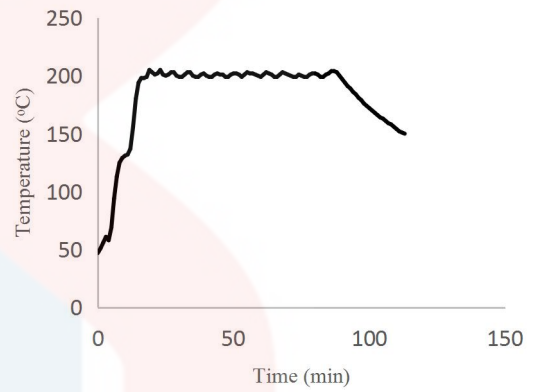


Table B.21: Burning phase experiment 13

Time	Temp.	Time	Temp.	Time	Temp.	Phase (min)
0	46	45	252	90	213	
1	49	46	253	91	208	
2	65	47	251	92	206	
3	93	48	249	93	204	
4	115	49	249	94	202	
5	128	50	251	95	200	
6	134	51	253	96	197	
7	136	52	252	97	195	
8	136	53	249	98	193	
9	136	54	249	99	191	
10	142	55	250	100	190	
11	162	56	252	101	188	
12	186	57	249	102	185	
13	198	58	250	103	183	
14	202	59	251	104	182	
15	202	60	249	105	177	
16	204	61	249	106	176	
17	218	62	250	107	174	
18	248	63	251			
19	251	64	252			
20	252	65	250			
21	253	66	250			
22	250	67	249			
23	250	68	250			
24	252	69	249			
25	253	70	250			
26	250	71	249			
27	247	72	246			
28	246	73	248			
29	252	74	250			
30	254	75	252			
31	252	76	249			
32	249	77	251			
33	248	78	252			
34	251	79	240			
35	253	80	236			
36	252	81	235			
37	249	82	234			
38	248	83	234			
39	250	84	231			
40	253	85	228			
41	253	86	224			
42	250	87	221			
43	248	88	218			
44	249	89	215			

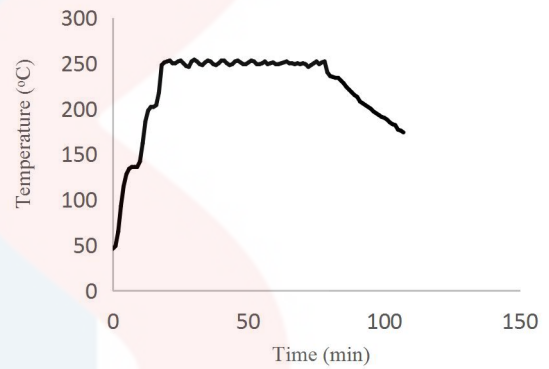


Table B.22: Burning phase experiment 14

Time	Temp.	Time	Temp.	Time	Temp.	Phase (min)
0	75	45	301	90	298	
1	87	46	298	91	294	
2	96	47	298	92	275	
3	101	48	301	93	270	
4	103	49	301	94	266	
5	109	50	298	95	262	
6	130	51	298	96	261	
7	154	52	302	97	257	
8	168	53	303	98	253	
9	173	54	300	99	251	
10	174	55	299	100	247	
11	174	56	302	101	242	
12	183	57	302	102	240	
13	206	58	299	103	238	
14	226	59	298	104	236	
15	234	60	299	105	233	
16	234	61	301	106	230	
17	251	62	302	107	228	
18	275	63	300	108	226	
19	286	64	298	109	224	
20	285	65	301	110	222	
21	287	66	303	111	221	
22	305	67	301	112	219	
23	302	68	298	113	218	
24	301	69	302	114	217	
25	300	70	300	115	215	
26	302	71	298	116	213	
27	299	72	301	117	212	
28	303	73	303	118	210	
29	305	74	301			
30	303	75	300			
31	298	76	300			
32	297	77	303			
33	299	78	298			
34	302	79	300			
35	305	80	302			
36	303	81	300			
37	299	82	299			
38	298	83	299			
39	302	84	300			
40	303	85	302			
41	301	86	301			
42	298	87	299			
43	298	88	300			
44	301	89	302			

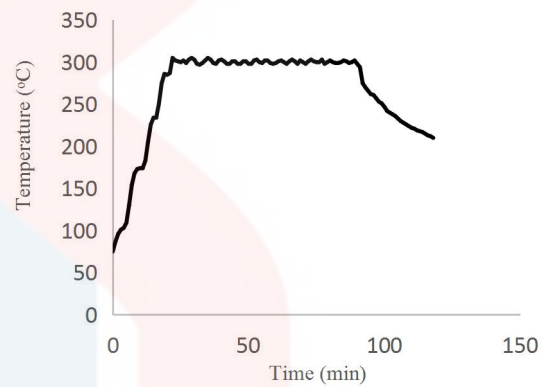


Table B.23: Burning phase experiment 15

Time	Temp.	Time	Temp.	Time	Temp.	Phase (min)
0	45	45	254	90	246	
1	45	46	252	91	243	
2	47	47	249	92	239	
3	53	48	249	93	236	
4	74	49	251	94	232	
5	118	50	253	95	228	
6	128	51	252	96	225	
7	131	52	249	97	222	
8	132	53	248	98	219	
9	132	54	251	99	217	
10	138	55	253	100	214	
11	159	56	252	101	212	
12	183	57	250	102	208	
13	195	58	249	103	206	
14	198	59	249	104	205	
15	197	60	252	105	202	
16	200	61	252	106	200	
17	218	62	250	107	198	
18	242	63	248	108	195	
19	253	64	250	109	193	
20	254	65	248	110	192	
21	252	66	250	111	190	
22	251	67	252	112	188	
23	252	68	252	113	187	
24	250	69	251	114	185	
25	248	70	248			
26	249	71	249			
27	251	72	251			
28	253	73	251			
29	251	74	253			
30	248	75	252			
31	248	76	251			
32	251	77	248			
33	254	78	249			
34	254	79	251			
35	253	80	253			
36	249	81	252			
37	248	82	250			
38	250	83	248			
39	253	84	248			
40	252	85	249			
41	250	86	249			
42	248	87	251			
43	249	88	251			
44	252	89	249			

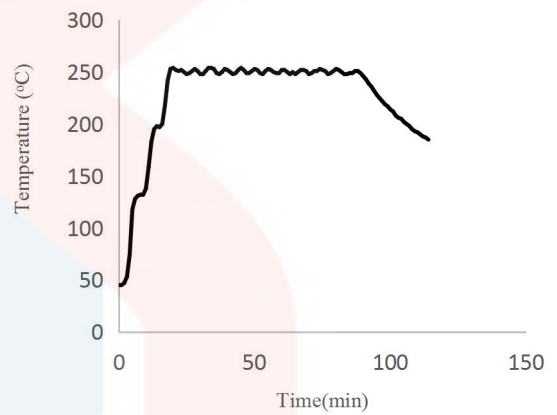
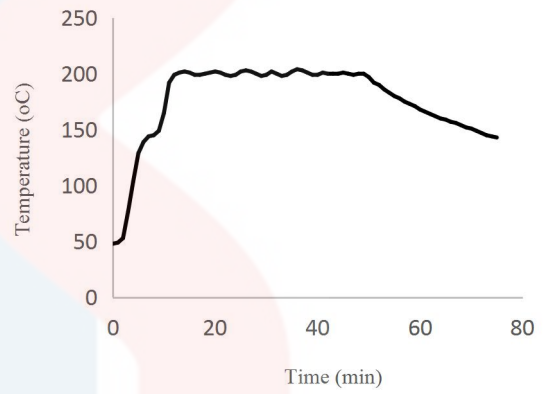


Table B.24: Burning phase experiment 16

Time	Temp.	Time	Temp.	Time	Temp.	Phase (min)
0	49	45	298	90	298	
1	52	46	299	91	300	
2	74	47	302	92	303	
3	114	48	302	93	302	
4	137	49	299	94	299	
5	147	50	298	95	299	
6	151	51	299	96	301	
7	152	52	302	97	302	
8	150	53	303	98	300	
9	149	54	300	99	299	
10	152	55	298	100	299	
11	170	56	299	101	301	
12	196	57	301	102	302	
13	210	58	302	103	300	
14	215	59	301	104	299	
15	214	60	302	105	299	
16	215	61	301	106	301	
17	230	62	298	107	302	
18	254	63	299	108	300	
19	268	64	302	109	299	
20	270	65	303	110	299	
21	269	66	301	111	300	
22	278	67	298	112	299	
23	301	68	299	113	300	
24	300	69	302	114	298	
25	301	70	303	115	299	
26	302	71	301	116	301	
27	300	72	298	117	302	
28	301	73	299	118	300	
29	304	74	300	119	297	
30	302	75	301	120	293	
31	299	76	303	121	289	
32	298	77	301	122	280	
33	302	78	299	123	276	
34	304	79	301	124	272	
35	300	80	298	125	269	
36	297	81	301	126	265	
37	298	82	303	127	262	
38	303	83	302	128	259	
39	300	84	299	129	256	
40	298	85	298	130	253	
41	299	86	300	131	251	
42	302	87	302	132	248	
43	300	88	301	133	245	
44	300	89	299	134	243	

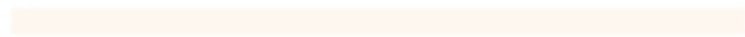
Table B.25: Burning phase experiment 17

Time	Temp.	Time	Temp.	Time	Temp.	Phase (min)
0	48	45	201			
1	49	46	200			
2	53	47	199			
3	77	48	200			
4	104	49	200			
5	129	50	197			
6	139	51	192			
7	144	52	190			
8	145	53	186			
9	149	54	183			
10	165	55	180			
11	192	56	178			
12	199	57	175			
13	201	58	173			
14	202	59	171			
15	201	60	168			
16	199	61	166			
17	199	62	164			
18	200	63	162			
19	201	64	160			
20	202	65	159			
21	201	66	157			
22	199	67	156			
23	198	68	154			
24	199	69	152			
25	202	70	151			
26	203	71	149			
27	202	72	147			
28	200	73	145			
29	198	74	144			
30	199	75	143			
31	202					
32	200					
33	198					
34	199					
35	202					
36	204					
37	203					
38	201					
39	199					
40	199					
41	201					
42	200					
43	200					
44	200					

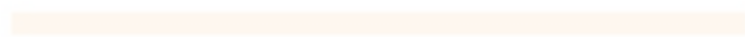




UNIVERSITI



MALAYSIA



KELANTAN